(1.08 ml, 14.7 mmol), and $NaBH_3CN$ (90%, 117 mg, 1.68 mmol) were added at 0 °C and the mixture was stirred at room temperature for 73 h. Ten percent aqueous KOH (2.0 ml) was added to pH 8–9 and the whole was extracted with $CH_2Cl_2$ (1 × 5 ml, 1 × 3 ml, 2 × 2 ml). The combined organic layer was washed with brine and was dried over $K_2CO_3$. The solvent was evaporated in vacuo and the residue was purified by column chromatography (NH silica, benzene:AcOEt:MeOH = 20:2:0.75) to give a reddish brown oil (86 mg, 76%); IR (ATR, $cm^{-1}$) 3200; $^1H$ NMR (400 MHz, $CDCl_3$) $\delta$ (ppm): 1.05 (6H, d, $J$ = 6.2 Hz, 2 × $CH_3$), 2.82 (1H, quint. $J$ = 6.2 Hz, CH), 2.94 (4H, s, 2 × $CH_2$), 3.85 (3H, s, $OCH_3$), 6.85 (1H, dd, $J$ = 8.8, 2.4 Hz, H-6), 6.98 (1H, d, $J$ = 2.4 Hz, H-4), 7.06 (1H, d, $J$ = 2.4 Hz, H-2), 7.13 (1H, d, $J$ = 8.8 Hz, H-7), 8.51 (1H, s, NH, exchangeable with $D_2O$); $^{13}C$ NMR (125 MHz, $CDCl_3$) $\delta$ (ppm): 22.8, 25.9, 47.4, 48.5, 55.9, 100.7, 111.8, 112.0, 113.4, 122.8, 129.8, 131.6, 153.7; HREIMS found: 232.1555 (calculated for $C_{13}H_{18}N_2O$:232.1575). These analytical data supported the conclusion that the synthesized compound was isopropyl-[2-(5-methoxy-1H-indol-3-yl)ethyl]amine (5-methoy-N-isopropyltryptamine, 5-MeO-IPT) (Fig. 1).

### 2.3. Construction of CYP expression plasmids

CYP1A2 cDNA for subcloning in expression vector pGYR1 was prepared by polymerase chain reaction (PCR) from pcDNA3.1/CYP1A2 plasmid [7] as a template using the forward primer, 5′-AAGCTTAAAAAAATGGCATTGTCCCAGTCT-3′, and the reverse primer, 5′-AAGCTTTCAGTTGATGGAGAAGCGCA-3′. The *Hin*dIII sites (marked with the solid lines) were introduced to the 5′-end of the start codon and the 3′-end of the stop codon to facilitate subcloning into pGYR1. A Kozak sequence (marked in italics) was also introduced upstream of the start codon to achieve high expression of the protein in yeast cells. CYP2C8 and CYP2C9 cDNAs were amplified from human adult normal liver QuickClone cDNA (BD Biosciences Clontech, Mountain View, CA). The nucleotide sequences used for the forward and reverse primers were 5′-CCCAAGCTTAAAAAAATGGAACCTTTTGTGGTCCTGG-3′ and 5′-TTCAAGCTTCTCGAGTTCAGACAGGGATGAAGCA-GAT-3′ for CYP2C8, and 5′-AAGCTTAAAAAAATGGATTCTC-TTGTGGTC-3′ and 5′-AAGCTTTCAGACAGGAATGAAGCACA-3′ for CYP2C9. The PCR products were directly introduced into pGEM-T vector (Promega, Madison, WI) using the TA cloning system, resulting in pGEM-T/CYP1A2, pGEM-T/CYP2C8 and pGEM-T/CYP2C9. CYP2C19 cDNA cloned into pBluescript SK (±) (pBluescript/CYP2C19) was supplied by Dr. J. Goldstein (NIEHS, Research Triangle, NC). The cDNA containing the *Hin*dIII sites and Kozak sequence was amplified by PCR from pcDNA3.1/CYP2C19 as a template using the forward primer 5′-CCCAAGCT-TAAAAAAATGGATCCTTTTGTGGTCC-3′ and the reverse primer 5′-GGAAAGCTTAGGAGCAGCCAGACCATCTGT-3′. The PCR product was digested with *Hin*dIII and ligated into the same restriction enzyme site of pcDNA3.1 (+), resulting in pcDNA3.1/CYP2C19. pGEM-T/CYP1A2, pGEM-T/CYP2C8, pGEM-T/CYP2C9 and pcDNA3.1/CYP2C19 plasmids were sequenced in both the forward and reverse directions using ABI BigDye terminator cycle sequencing reaction kit v3.1 (Applied Biosystems, Piscaway, NJ) to confirm that there were no PCR errors. The DNA fragments corresponding to CYP1A2, CYP2C8, CYP2C9 and CYP2C19 were cut out with *Hin*dIII from the pGEM-T or pcDNA3.1 (+) plasmid and were subsequently subcloned into the pGYR1 yeast expression vector digested with *Hin*dIII. The expression plasmids were sequenced to verify the correct orientation with respect to the promoter for pGYR1. The construction of CYP2D6 expression plasmid (pGYR1/CYP2D6) was described previously [8]. CYP3A4 expression plasmid (pGYR1/CYP3A4) was supplied by Dr. Y. Saito (National Institute of Health Sciences, Tokyo, Japan).

### 2.4. Expression of CYP enzymes

The pGYR1 vectors containing CYP cDNAs were used to transform *Saccharomyces cerevisiae* AH22 by the lithium acetate

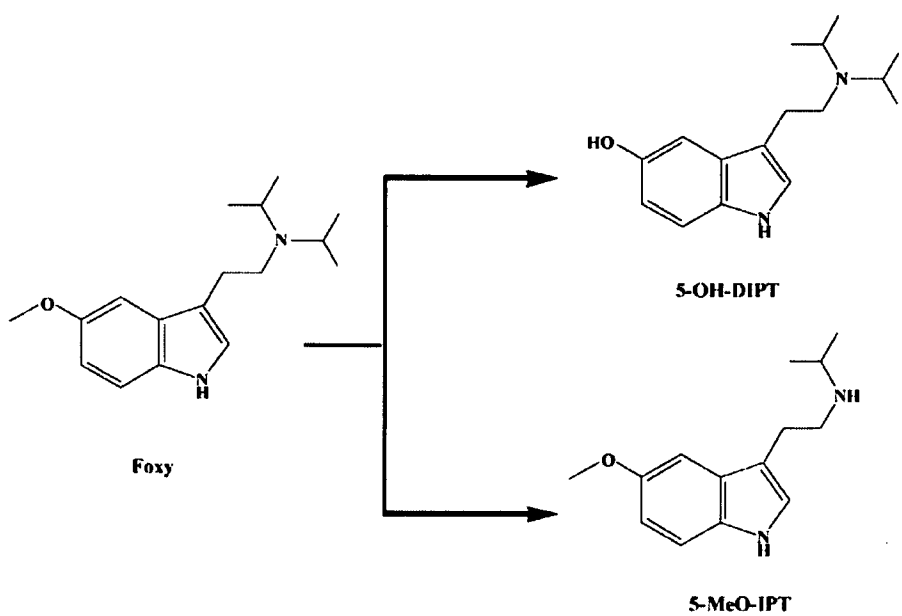


**Fig. 1 – Major metabolic pathways of 5-MeO-DIPT.**

method, and the cultivation of yeast transformants was performed as described [9]. Microsomes from yeast were prepared as described previously [10]. The yeast cell microsomal content of each recombinant CYP enzyme was as follows: CYP1A2 (13.5 pmol/mg protein), CYP2C8 (95.3 pmol/mg protein), CYP2C9 (76.0 pmol/mg protein), CYP2C19 (41.8 pmol/mg protein), CYP2D6 (65.0 pmol/mg protein) and CYP3A4 (49.1 pmol/mg protein).

### 2.5. *Measurement of oxidation activities of 5-MeO-DIPT*

A typical reaction mixture consisted of G-6-P (10 mM, final concentration), NADPH (1 mM), $MgCl_2$ (10 mM), EDTA (0.2 mM), microsomal fraction from human liver or yeast cells expressing CYP enzyme (0.08–0.12 mg protein) and the substrate (0.1–1000 μM) in 50 mM potassium phosphate buffer (pH 7.4) in a 1.5-ml Eppendorf-type tube (a final volume of 200 μl). Following preincubation at 37 °C for 5 min, the reaction was started by adding microsomal fractions from human livers or yeast cells expressing CYP enzymes, continued for 5–10 min, and stopped by adding aqueous 2 M phosphoric acid (10 μl) and 20 mM ascorbic acid (20 μl), vigorously mixing with a Vortex mixer, and chilling in an ice bath for 10 min. The tube was then centrifuged at 14,000 × *g* at 4 °C for 10 min, and the supernatant was passed through a 0.45-μm membrane filter (Millipore, Billerica, MA). An aliquot (20 μl) was subjected to high-performance liquid chromatography (HPLC) under the conditions described below. Calibration curves of 5-OH-DIPT and 5-MeO-IPT were made by spiking ice-cold reaction medium with known amounts of the synthetic compounds, followed by the addition of aqueous 2 M phosphoric acid and 20 mM ascorbic acid and treatment as described above. The detection limits for 5-OH-DIPT and 5-MeO-IPT were 0.5 and 1.0 pmol/ml, with a signal-to-noise ratio of 3 in both cases. The intra- and inter-day coefficients of variation did not exceed 10% for any assay.

### 2.6. *HPLC conditions*

The HPLC apparatus consisted of a Hitachi L-2130 pump, an L-2480 fluorescence detector, an L-2300 column oven, a D-2000 system manager (version 1.1) and a Rheodyne type 7725i injector. Other conditions were as follows: column, Inertsil C8 (150 mm × 4.6 mm i.d., GL Sciences, Co. Ltd., Tokyo, Japan); column temperature, 40 °C; detection, fluorescence excitation/emission wavelength, 280/340 nm. The mobile phase used was a linear gradient system consisting of (A) 20 mM ammonium acetate (pH 4.0)/acetonitrile (92:8 v/v) and (B) 20 mM ammonium acetate (pH 4.0)/acetonitrile (80:20) as follows: 0–3 min, (A) 100%; 3–15 min, from (A) 100% to (B) 100%; 15–25 min, (B) 100%; 25–30 min, from (B) 100% to (A) 100%; 30–40 min, (A) 100% at a flow rate of 0.9 ml/min.

### 2.7. *LC/MS conditions*

LC/MS analysis was performed using a JMS-700 MStation (JEOL, Tokyo, Japan). HPLC conditions were: column, Inertsil ODS-3 (150 mm × 2.1 mm i.d., GL Science); mobile phase, aqueous 0.1% TFA/acetonitrile (84:16 v/v); column temperature, 40°; flow rate, 0.2 ml/min; injection volume, 20 μl; detection, fluorescence excitation/emission wavelength, 280/340 nm. MS conditions were: ionization mode, ESI(+); needle voltage, 2.0 kV; ring voltage, 45 V; orifice voltage, 0 V; the temperatures of the orifice and desolvating plate were 80 and 220 °C; the resolution of the mass spectrometer was set at 1000 or 3000; collision gas, He.

### 2.8. *Others*

Total holo-CYP contents in yeast cell microsomal fractions were spectrophotometrically measured by assessing the reduced carbon monoxide spectra according to the method of Omura and Sato [11] using 91 $mM^{-1}$ $cm^{-1}$ as the absorption coefficient. Protein concentration was determined by the method of Lowry et al. [12]. Kinetic parameters (apparent $K_m$ and $V_{max}$ values) were estimated by analyzing Michaelis–Menten plots or Eadie–Hofstee plots using the computer program Prism ver. 4.0 software (GraphPad Software, San Diego, CA).

## 3. Results

First, we examined the in vitro oxidative metabolism of 5-MeO-DIPT using pooled human liver microsomes from Caucasians. When 50 μM 5-MeO-DIPT was used as the substrate, two major metabolite peaks [M – 1 (retention time of 10.3 min) and M – 3 (15.1 min)] were observed on the HPLC chromatogram (Fig. 2). Because the retention times and fragmentation profiles of M – 1 and M – 3 coincided with those of 5-OH-DIPT and 5-MeOH-IPT synthetic standards in LC/MS analysis, M – 1 and M – 3 were identified as 5-OH-DIPT and 5-MeOH-IPT, respectively (Fig. 3).

Furthermore, two metabolite peaks [M – 2 (retention time 12.0 min) and M – 4 (17.7 min) in HPLC] were analyzed by LC/MS. The fragment ions were as follows: M – 2; *m/z* 291 (M + 1, 100%), 181 (42%), 140 (85%), 124 (18%): M – 4; *m/z* 305 (M + 1, 64%), 278 (18%), 204 (55%), 144 (100%). From the molecular ion (*m/z* 291), M – 2 is thought to be a monohy-

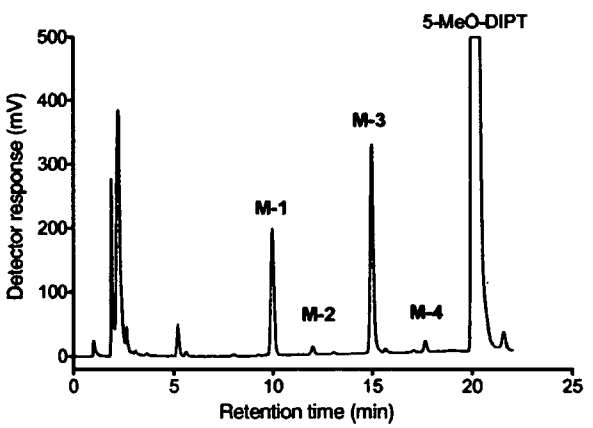


**Fig. 2 – A typical HPLC chromatogram of 5-MeO-DIPT and its metabolites. The reaction mixture containing human liver microsomes and 5-MeO-DIPT (50 μM) was incubated in the presence of an NADPH-generating system and the metabolites formed were examined by HPLC under the conditions described in Section 2.**

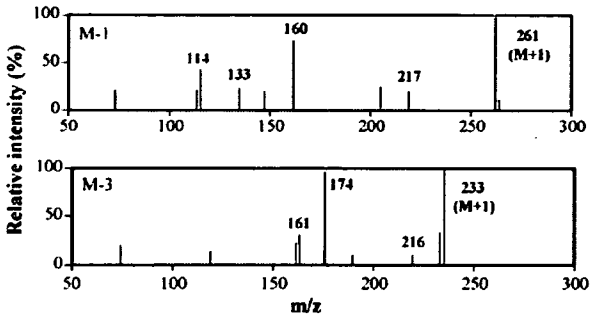


**Fig. 3 – Mass fragment ions of M – 1 and M – 3. LC/MS conditions are given in Section 2.**

droxylated 5-MeO-DIPT. It is feasible that M – 4 is a dehydrogenated product of dihydroxylated 5-MeO-DIPT.

It is reasonable to think that the formation of these metabolites was catalyzed by CYP enzymes in the liver microsomal fractions. We therefore examined what kinds of CYP enzymes were involved in the formation of M – 1 and M – 3 from 5-MeO-DIPT in human liver microsomes in the second step of this study. For this, we used six human recombinant CYP enzymes expressed in yeast cells: CYP1A2, CYP2C8, CYP2C9, CYP2C19, CYP2D6 and CYP3A4.

In this experiment, we employed two substrate concentrations (1 and 50 μM). All of the CYP enzymes except for CYP3A4 exhibited the capacity to oxidize 5-MeO-DIPT (Fig. 4). CYP3A4 expressed in yeast cells did not produce any metabolites in detectable amounts even at 50 μM substrate under the conditions used. We further examined the metabolic capacity of commercially available insect cell microsomal fractions (Supersomes) expressing CYP3A4, OR and cytochrome $b_5$. Interestingly, Supersomes co-expressing CYP3A4 with cytochrome $b_5$ exhibited considerable 5-MeO-DIPT N-deisopropylase but not O-demethylase activity, whereas Supersomes without cytochrome $b_5$ did not show any detectable activity (Fig. 4). As a result, among the six CYP enzymes tested, only CYP2D6 exhibited 5-MeO-DIPT O-demethylase activity, whereas all of the six recombinant enzymes showed 5-MeO-DIPT N-deisopropylase activitiy. The activities were ranked as CYP2C19 > CYP1A2 > CYP3A4 > CYP2C8 > CYP2C9 = CYP2D6.

Table 1 – Kinetic parameters for 5-MeO-DIPT oxidation by human liver microsomes

| | $K_m$ (μM) | $V_{max}$ (pmol/min/mg protein) | $V_{max}/K_m$ (μl/min/mg protein) |
|---|---|---|---|
| O-demethylation | 5.0 | 140 | 27.9 |
| N-deisopropylation | | | |
| Low-$K_m$ phase | 24 | 25 | 1.03 |
| Intermediate-$K_m$ phase | 257 | 178 | 0.69 |
| High-$K_m$ phase | 1201 | 409 | 0.34 |

Each value represents the mean of two determinations.

We then performed kinetic analysis using substrate concentrations ranging from 0.1 to 1000 μM and the pooled human microsomal fraction and the yeast cell microsomal fractions expressing recombinant CYP enzymes as enzyme sources. Only for CYP3A4, the Supersomes expressing CYP3A4, OR and cytochrome $b_5$ was employed. 5-MeO-DIPT O-demethylation by the pooled human liver microsomal fraction exhibited monophasic kinetics (Fig. 5A), whereas human liver microsomal N-deisopropylation showed triphasic kinetics (Fig. 5B). Table 1 summarizes the kinetic parameters. The apparent $K_m$ value for monophasic 5-MeO-DIPT O-demethylation was calculated to be 5 μM, while the low-, intermediate- and high-$K_m$ values for triphasic N-deisopropylation were calculated to be 24, 260 and 1200 μM, respectively.

For 5-MeO-DIPT O-demethylation, recombinant CYP2D6 yielded monophasic kinetics and an apparent $K_m$ value of 2 μM. For 5-MeO-DIPT N-deisopropylation, CYP2C19, CYP3A4, CYP1A2, CYP2C8 and CYP2C9 showed monophasic kinetics, and gave $K_m$ values of 35, 180, 260, 290 and 1660 μM, respectively (Table 2). These $K_m$ values are similar to the values of the low-, intermediate- and high-$K_m$ phases, respectively, of the human liver microsomal fraction (Table 1). In the case of N-

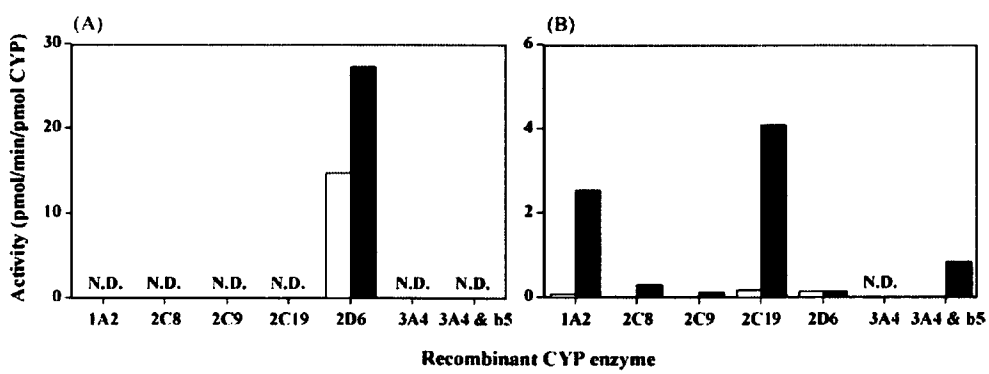


**Fig. 4 – Comparison of 5-MeO-DIPT oxidation activities of recombinant CYP enzymes expressed in yeast or insect cells. For incubation, 5 pmol of each CYP enzyme was employed: (A) 5-MeO-DIPT O-demethylation; (B) 5-MeO-DIPT N-deisopropylation. Open columns, 5-MeO-DIPT 1 μM; closed columns, 5-MeO-DIPT 50 μM. Each value represents the mean of two determinations. 3A4 & $b_5$, Supersomes; N.D., not detectable.**

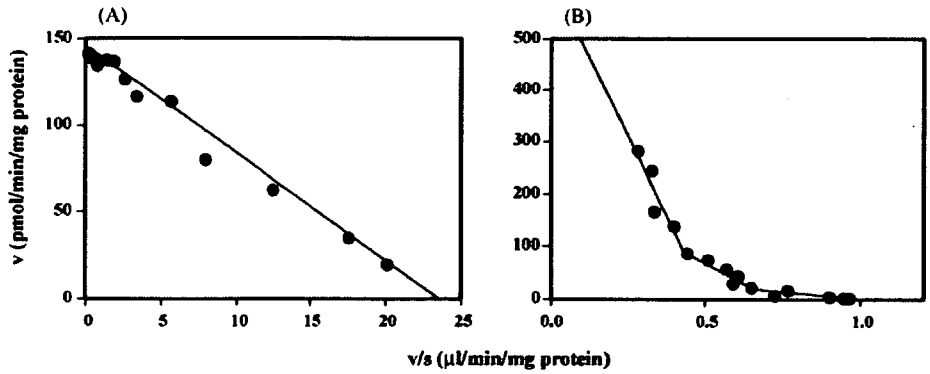


**Fig. 5 – Kinetic analysis of 5-MeO-DIPT oxidation by human liver microsomes. (A) and (B) Eadie–Hofstee plots for 5-MeO-DIPT O-demethylation and N-deisopropylation, respectively.**

deisopropylation by CYP2D6, precise kinetic parameters were not calculated because of the low activities.

In the third step of the present study, we examined the effects of inhibitors of the CYP enzymes on the oxidative metabolism of 5-MeO-DIPT in human liver microsomes to estimate the contribution of the CYP enzymes. For this, we employed furafylline [13], quercetin [14], sulfaphenazole [15], omeprazole [16], quinidine [17] and ketoconazole [18] as specific inhibitors of CYP1A2, CYP2C8, CYP2C9, CYP2C19, CYP2D6 and CYP3A4, respectively. For 5-MeO-DIPT O-demethylation by human liver microsomes, quinidine showed a concentration-dependent inhibition. Over 95% of the activity was suppressed by the inhibitor even at 5 μM (Fig. 6A).

Furafylline and quercetin inhibited human liver microsomal 5-MeO-DIPT N-deisopropylation in a concentration-dependent manner, but about 30–40% of the activity remained even at the highest concentration of the inhibitors (Fig. 6B and C). Sulfaphenazole also caused a concentration-dependent

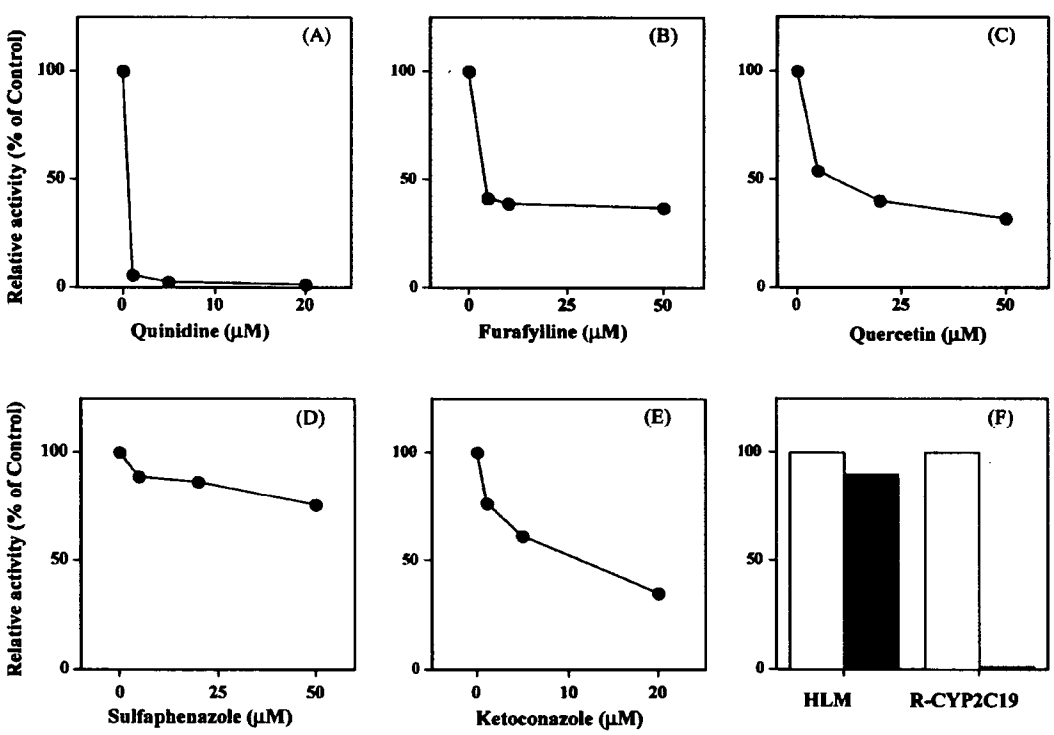


**Fig. 6 – Effects of various CYP inhibitors on 5-MeO-DIPT oxidation by human liver microsomes: (A) quinidine (0, 0.5, 5 and 20 μM) as CYP2D6 inhibitor; (B) furafylline (0, 5, 10 and 50 μM) as CYP1A2 inhibitor; (C) quercetin (0, 5, 20 and 50 μM); (D) sulfaphenazole (0, 5, 20 and 50 μM) as CYP2C9 inhibitor; (E) ketoconazole (0, 1, 5 and 20 μM) as CYP3A4 inhibitor; (F) omeprazole (10 μM) as CYP2C19 inhibitor. (A) 5-MeO-DIPT O-demethylation; (B), (C), (D), (E) and (F) 5-MeO-DIPT N-deisopropylation. The substrate concentrations used were 10 μM for (A) and 50 μM for (B), (C), (D), (E) and (F). Each value represents the mean of two determinations. HLM, human liver microsomes.**

Table 2 – Kinetic parameters for 5-MeO-DIPT oxidation by recombinant CYP enzymes expressed in yeast cells

| | $K_m$ (μM) | $V_{max}$ (pmol/min/pmol CYP) | $V_{max}/K_m$ (μl/min/pmol CYP) |
|---|---|---|---|
| O-demethylation | | | |
| CYP2D6 | 2.0 | 29.8 | 14.8 |
| N-deisopropylation | | | |
| CYP1A2 | 263 | 9.4 | 0.04 |
| CYP2C8 | 291 | 1.7 | 0.006 |
| CYP2C9 | 1663 | 4.2 | 0.003 |
| CYP2C19 | 35 | 6.9 | 0.19 |
| CYP3A4[a] | 184 | 4.4 | 0.02 |

Each value represents the mean of two determinations.
[a] Data from Supersomes in which CYP3A4 and cytochrome $b_5$ were co-expressed.

inhibition, but suppressed only 25% of human liver microsomal 5-MeO-DIPT N-deisopropylation at the highest concentration of 50 μM (Fig. 6D). Ketoconazole suppressed 40% and 65% of the N-deisopropylase activity at final concentrations of 5 and 20 μM, respectively (Fig. 6E). Omeprazole (10 μM) suppressed only 10% of 5-MeO-DIPT N-deisopropylation by pooled human liver microsomes, though this inhibitor at the same concentration suppressed the 5-MeO-DIPT N-deisopropylation by recombinant CYP2C19 almost completely (Fig. 6F).

## 4. Discussion

There have hitherto been no reports of the quantitative assays using authentic samples of 5-MeO-DIPT metabolites to study the formation of 5-MeO-DIPT metabolites. We therefore chemically synthesized the two compounds, 5-OH-DIPT and 5-MeO-IPT, and conducted a quantitative analysis of the formation of these metabolites. Using these synthetic samples, we examined the in vitro oxidative metabolism of 5-MeO-DIPT by human liver microsomes and recombinant CYP enzymes. As expected, 5-MeO-DIPT was biotransformed into 5-OH-DIPT and 5-MeO-IPT as major metabolites by human liver microsomes under the conditions used. Two other metabolites were also tentatively identified as monohydroxylated 5-MeO-DIPT and a dehydrogenated product of dihydroxylated 5-MeO-DIPT on the basis of the data from LC/MS analysis.

In a preliminary HPLC experiment, we compared the amounts of 5-OH-DIPT and 5-MeO-IPT formed with the amount of 5-MeO-DIPT consumed during the incubation of the substrate (10 μM) under similar conditions to those employed here. The results indicated that at least 95% of substrate consumption was explained by the formation of the two major metabolites (data not shown). Therefore, it is reasonable to think that 5-OH-DIPT and 5-MeO-IPT are the major metabolites in human liver microsomes at around 10 μM substrate concentrations (Fig. 1).

Human liver microsomal 5-MeO-DIPT O-demethylation and N-deisopropylation exhibited monophasic and triphasic kinetics, respectively. We have been studying the relationships between protein structures and enzymatic functions of major drug-metabolizing CYP enzymes such as CYP1A2 [19] and CYP2D6 [20,21]. Using the yeast cell expression systems of CYP1A2, CYP2C8, CYP2C9, CYP2C19, CYP2D6 and CYP3A4 constructed so far in this laboratory, we examined the metabolic capacities of these recombinant enzymes for the oxidation of 5-MeO-DIPT.

Among the recombinant enzymes, only CYP2D6 showed considerable 5-MeO-DIPT O-demethylase activity. This reaction in human liver microsomes yielded monophasic kinetics, and was almost completely suppressed by quinidine as a specific inhibitor of CYP2D6. The apparent $K_m$ value (2 μM) for the recombinant CYP2D6 was similar to that (5 μM) for the human liver microsomes. These results indicate that 5-MeO-DIPT O-demethylation was mainly mediated by CYP2D6 in human livers.

In contrast, the two CYP enzymes (CYP1A2 and CYP2C19) in the yeast cell expression system exhibited considerable 5-MeO-DIPT N-deisopropylase activities. The activities of CYP2C8, CYP2C9 and CYP2D6 were much lower than those of CYP1A2 and CYP2C19. Interestingly, yeast cell microsomal CYP3A4 did not show any detectable activity for either O-demethylation or N-deispropylation. Before coming to a conclusion, we further examined the metabolic capacity of Supersomes expressing CYP3A4, OR and cytochrome $b_5$, because it is well known that co-existence of cytochrome $b_5$ increases the oxidation capacity of CYP3A4 for its substrates [22,23]. As expected, Supersomes co-expressing CYP3A4 with cytochrome $b_5$ exhibited considerable 5-MeO-DIPT N-demethylase activity, whereas Supersomes without cytochrome $b_5$ did not.

The apparent $K_m$ values for CYP2C19 (35 μM), CYP3A4 (180 μM), CYP1A2 (260 μM), CYP2C8 (290 μM) and CYP2C9 (1700 μM) seem to correspond to those for human liver microsomal low- (24 μM), intermediate- (260 μM) and high-$K_m$ (1200 μM) phases, respectively. To confirm the involvement of these CYP enzymes in human liver microsomal 5-MeO-DIPT N-deisopropylation, the effects of furafylline, quercetin, sulfaphenazole, omeprazole and ketoconazole were examined as specific inhibitors for CYP1A2, CYP2C8, CYP2C9, CYP2C19 and CYP3A4, respectively. Among them, furafylline, quercetin and ketoconazole exerted considerable inhibitory effects at relatively low concentrations (several μM).

We employed quercetin as the inhibitor of CYP2C8 in the present study, however, this compound was reported to inhibit the metabolic activities of CYP1A2, CYP2C19 and CYP3A4 as well [24]. Therefore, quercetin could suppress the activities not only of CYP2C8 but also of CYP1A2 and CYP3A4 in 5-MeO-DIPT N-deisopropylation by human liver microsomal fraction in this study. Inhibitory effect of sulfaphenazole was found to be weak as compared to those of furafylline and ketoconazole. Interestingly, the inhibitory effect of omeprazole was very weak under the conditions used. In this case, we employed an inhibitor concentration of 10 μM, which was sufficient to suppress the bufuralol 1″-hydroxylase activities of CYP2C19 in our previous studies [25]. In fact, 10 μM omeprazole completely suppressed 5-MeO-DIPT N-deisopropylation by recombinant CYP2C19 in the present study.

Other drug-metabolizing-type CYP enzymes such as CYP2E1, CYP2A6 and CYP2B6 could also be involved in the oxidation of 5-MeO-DIPT in the human liver. In another

preliminary experiment, we found that diethyldithiocarbamate (5, 20 and 100 μM final concentrations) as CYP2E1 inhibitor [26] did not affect 5-MeO-DIPT oxidation by the pooled human liver microsomal fraction (data not shown). Ono et al. [27] reported that diethyldithiocarbamate inhibits the metabolic activities of CYP2A6 and CYP2C19 in addition to that of CYP2E1. Furthermore, furafylline and ketoconazole (5 μM each) suppressed 60% and 40%, respectively, of human liver microsomal 5-MeO-DIPT *N*-deisopropylation under the conditions employed. CYP3A4 is the most abundant CYP enzyme followed by CYP2C and CYP1A2 in the human liver [28]. These results indicate that CYP1A2, CYP2C8 and CYP3A4 are the major 5-MeO-DIPT *N*-deisopropylases in the human liver at substrate concentrations around 50 μM or less.

The present results of the measurement of enzyme activities and the effects of inhibitors indicated that human liver microsomal 5-MeO-DIPT *O*-demethylation is mainly mediated by CYP2D6, whereas *N*-deisopropylation is mediated mainly by CYP1A2 and CYP3A4, and also by CYP2C8, CYP2C9 and CYP2C19, at least in part. The major contribution of CYP2D6 to 5-MeO-DIPT *O*-demethylation is predictable from the previous findings of Yu et al. [29,30] on the role of CYP2D6 in 5-MeO-tryptamine metabolism. It should be noted that though CYP2C19 exhibited the highest activity as 5-MeO-DIPT *N*-deisopropylase among the six recombinant CYP enzymes examined, its contribution was thought to be relatively low in the reaction by the pooled human liver microsomal fractions used in the present study.

The kinetic parameters, particularly the clearance ($V_{max}/K_m$) values, indicate that as compared to *N*-deisopropylation, *O*-demethylation might contribute to a much greater extent to the oxidative metabolism of 5-MeO-DIPT. The present results together with previous in vivo and in vitro findings cast considerable light on the metabolic fate of 5-MeO-DIPT in the human body. However, the toxicity of 5-MeO-DIPT and related compounds, including the metabolites of 5-MeO-DIPT, remain to be elucidated. If only the parent compound, 5-MeO-DIPT, has psychotomimetic activity and 5-MeO-DIPT *O*-demethylation is mediated mainly by CYP2D6, poor metabolizers who are deficient for functional CYP2D6 may show higher sensitivity to, or toxicity of, 5-MeO-DIPT than extensive metabolizers having normal CYP2D6 functions. Further systematic studies will be needed to understand the relationship between the metabolism and toxicity of 5-MeO-DIPT.

In summary, in vitro quantitative studies on the oxidative metabolism of 5-MeO-DIPT were performed using human liver microsomal fractions, recombinant CYP enzymes and synthetic 5-MeO-DIPT metabolites. 5-MeO-DIPT was mainly oxidized to *O*-demethylated (5-OH-DIPT) and *N*-deisopropylated (5-MeO-IPT) metabolites in pooled human liver microsomes. Kinetic analysis revealed that 5-MeO-DIPT *O*-demethylation showed monophasic kinetics, whereas *N*-deisopropylation gave triphasic kinetics. Among the six recombinant CYP enzymes examined, only CYP2D6 exhibited 5-MeO-DIPT *O*-demethylase activity, and CYP1A2, CYP2C8, CYP2C9, CYP2C19 and CYP3A4 showed 5-MeO-DIPT *N*-deisopropylase activities. The apparent $K_m$ value of CYP2D6 was close to that for 5-MeO-DIPT *O*-demethylation, and the $K_m$ value of other CYP enzymes were similar to those of the low-$K_m$ (CYP2C19), intermediate-$K_m$ (CYP1A2, CYP2C8 and CYP3A4) and high-$K_m$ (CYP2C9) phases, respectively, for *N*-deisopropylation in human liver microsomes. These results together with the results of the inhibitory studies indicate that CYP2D6 is the major 5-MeO-DIPT *O*-demethylase and CYP1A2, CYP2C8 and CYP3A4 are the major *N*-deisopropylase enzymes in the human liver.

## Acknowledgments

We would like to express our gratitude to Dr. Joyce A. Goldstein, National Institutes of Environmental Health Sciences, Research Triangle Park, NC, for her kind gift of CYP2C19 cDNA. This study was supported in part by a grant from the Japan Research Foundation for Clinical Pharmacology.

## REFERENCES

[1] Ishida T, Kudo K, Kiyosghima A, Inoue H, Tsuji A, Ikeda N. Sensitive determination of alfa-methyltryptamine (AMT) and 5-methoxy-*N*,*N*-diisopropyltryptamine (5MeO-DIPT) in whole blood and urine using gas chromatography–mass spectrometry. J Chromatogr B 2005;823:47–52.
[2] Kikura-hanajiri R, Hayashi M, Saisho K, Goda Y. Simultaneous determination of nineteen hallucinogenic tryptamines/β-calbolines and phenethylamines usig gas chromatography–mass spectrometry and liquid chromatography–electrospray ionization-mass spectrometry. J Chromatogr B 2005;825:29–37.
[3] Shulgin AT, Carter MF. *N*,*N*-diisopropyltryptamine (DIPT) and 5-methoxy-*N*,*N*-diisopropyltryptamine (5-MeO-DIPT), two orally active tryptamine analogs with CNS activity. Commun Psychopharmacol 1980;4:363–9.
[4] Meatherall R, Sharma P. Foxy, a designer tryptamine hallucinogen. J Anal Toxicol 2003;27:313–7.
[5] Wilson JM, McGeorge F, Smalinske S, Meatherall R. A foxy intoxication. Forensic Sci Int 2005;148:31–6.
[6] Tsuzuki D, Takemi C, Yamamoto S, Tamagake K, Imaoka S, Funae Y, et al. Functional evaluation of cytochrome P450 2D6 with Gly42Arg substitution expressed in *Saccharomyces cerevisiae*. Pharmacogenetics 2001;11: 709–18.
[7] Saito Y, Hanioka N, Maekawa K, Isobe T, Tsuneto Y, Nakamura R, et al. Functional analysis of three CYP1A2 variants found in a Japanese population. Drug Metab Dispos 2006;33:1905–10.
[8] Sakaki T, Akiyoshi-Shibata M, Yabusaki Y, Ohkawa H. Organella-targeted expression of rat liver cytochrome P450c27 in yeast: genetically engineered alteration of mitochondrial P450 into a microsomal form creates a novel functional electron transport chain. J Biol Chem 1992;267:16497–502.
[9] Wan J, Imaoka S, Chow T, Hiroi T, Yabusaki Y, Funae Y. Expression of four rat CYP2D isoforms in *Saccharomyces cerevisiae* and their catalytic specificity. Arch Biochem Biophys 1997;348:383–90.
[10] Hichiya H, Takemi C, Tsuzuki D, Yamamoto S, Asaoka A, Suzuki S, et al. Complementary DNA cloning and characterization of cytochrome P450 2D29 from Japanese monkey liver. Biochem Pharmacol 2002;64:1101–10.
[11] Omura T, Sato R. The carbon monoxide-binding pigment of liver microsomes. I. Evidence for its hemoprotein nature. J Biol Chem 1964;239:2370–8.

[12] Lowry OH, Rosebrough NJ, Farr AL, Randall RJ. Protein measurement with the Folin phenol reagent. J Biol Chem 1951;193:265–75.
[13] Sesardic D, Boobis AR, Murray BP, Murray S, Segura J, Torre R, et al. Furafylline is a potent and selective inhibitor of cytochrome P450IA2 in man. Br J Clin Pharmacol 1990; 29:651–63.
[14] Rahman A, Korzekwa KR, Grogan J, Gonzalez FJ, Harris JW. Selective biotransformation of taxol to 6α-hydroxytaxol by human cytochrome P450 2C8. Cancer Res 1994;54:5543–6.
[15] Mancy A, Dijols S, Poli S, Guengerich P, Mansuy D. Interaction of sulfaphenazole derivatives with human liver cytochromes P450 2C: molecular origin of the specific inhibitory effects of sulfaphenazole on CYP 2C9 and consequences for the substrate binding site topology of CYP 2C9. Biochemistry 1996;35:16205–12.
[16] Ko JW, Sukhova N, Thacker D, Chen P, Flockhart DA. Evaluation of omeprazole and lansoprazole as inhibitors of cytochrome P450 isoforms. Drug Metab Dispos 1997;25: 853–62.
[17] Newton DJ, Wang RW, Lu AY. Cytochrome P450 inhibitors. Evaluation of specificities in the in vitro metabolism of therapeutic agents by human liver microsomes. Drug Metab Dispos 1995;23:154–8.
[18] Schmider J, Greenblatt DJ, von Moltke LL, Harmatz JS, Shader RI. N-demethylation of amitriptyline in vitro: role of cytochrome P-450 3A (CYP3A) isoforms and effect of metabolic inhibitors. J Pharmacol Exp Ther 1995;275:592–7.
[19] Narimatsu S, Oda M, Hichiya H, Isobe T, Asaoka K, Hanioka N, et al. Molecular cloning and functional analysis of cytochrome P450 1A2 from Japanese monkey liver: Comparison with marmoset cytochrome P450 1A2. Chem Biol Interact 2005;152:1–12.
[20] Masuda K, Hashimoto H, Tamagake K, Okuda Y, Tsuzuki D, Isobe T, et al. Changes in the enzymatic properties of CYP2D6 by the substitution of phenylalanine at position 120 by alanine. J Health Sci 2004;50:503–10.
[21] Masuda K, Tamagake K, Okuda Y, Torigoe F, Tsuzuki D, Isobe T, et al. Change in enantioselectivity in bufuralol 1″-hydroxylation by the substitution of phenylalanine-120 by alanine in cytochrome P450 2D6. Chirality 2005;17:34–7.
[22] Yamazaki H, Johnson WW, Ueng YF, Shimada T, Guengerich FP. Lack of electron transfer from cytochrome $b_5$ in stimulation of catalytic activities of cytochrome P450 3A4. Characterization of a reconstituted cytochrome P450 3A4/NADPH-cytochrome P450 reductase system and studies with apo-cytochrome $b_5$. J Biol Chem 1996;271:27438–44.
[23] Jushchyshyn MI, Hutzler JM, Schrag ML, Wienkers LC. Catalytic turnover of pyrene by CYP3A4: evidence that cytochrome $b_5$ directly induces positive cooperativity. Arch Biochem Biophys 2005;438:21–8.
[24] Zou L, Harkey MR, Henderson GL. Effects of herbal components on cDNA-expressed cytochrome P450 enzyme catalytic activity. Life Sci 2002;71:1579–89.
[25] Narimatsu S, Takemi C, Tsuzuki D, Kataoka H, Yamamoto S, Shimada S, et al. Stereoselective metabolism of bufuralol racemate and enantiomers in human liver microsomes. J Pharmacol Exp Ther 2002;303:172–8.
[26] Yamazaki H, Oda Y, Funae Y, Imaoka S, Inui Y, Guengerich FP, et al. Participation of rat liver cytochrome P450 2E1 in the activation of *N*-nitrosodimethylamine and *N*-nitrosodiethylamine to products genotoxic in an acetyltransferase-overexpressing *Salmonella typhimurium* strain. Carcinogenesis 1992;13: 979–85.
[27] Ono S, Hatanaka T, Hotta H, Satoh T, Gonzalez FJ, Tsutsui M. Specificity of substrate and inhibitor probes for cytochrome P450s: evaluation of in vitro metabolism using cDNA-expressed human P450s and human liver microsomes. Xenobiotica 1996;26:681–93.
[28] Shimada T, Yamazaki H, Mimura M, Inui Y, Guengerich FP. Interindividual variations in human liver cytochrome P-450 enzymes involved in the oxidation of drugs, carcinogens and toxic chemicals: studies with liver microsomes of 30 Japanese and 30 Caucasians. J Pharmacol Exp Ther 1994;270:414–23.
[29] Yu AM, Idle JR, Byrd LG, Krausz KWA, Kupfer A, Gonzalez FJ. Regeneration of serotonin from 5-methoxytryptamine by polymorphic human CYP2D6. Pharmacogenetics 2003;13:173–81.
[30] Yu AM, Idle JR, Herraiz T, Kupfer A, Gonzalez FJ. Screening for endogenous substrates reveals that CYP2D6 is a 5-methoxyindolethylamine O-demethylase. Pharmacogenetics 2003;13:307–9.

BIOCHEMICAL PHARMACOLOGY 72 (2006) 1738–1748

available at www.sciencedirect.com

ScienceDirect

journal homepage: www.elsevier.com/locate/biochempharm

# Cloning of a cDNA encoding a novel marmoset CYP2C enzyme, expression in yeast cells and characterization of its enzymatic functions

*Shizuo Narimatsu*[a,*], *Fumihiro Torigoe*[a], *Yumi Tsuneto*[a], *Keita Saito*[a], *Nobumitsu Hanioka*[a], *Kazufumi Masuda*[b], *Takashi Katsu*[b], *Shigeo Yamamoto*[c], *Shigeru Yamano*[d], *Takahiko Baba*[e], *Atsuro Miyata*[f]

[a] *Laboratory of Health Chemistry, Graduate School of Medicine, Dentistry and Pharmaceutical Sciences, Okayama University, 1-1-1 Tsushima-naka, Okayama 700-8530, Japan*

[b] *Laboratory of Pharmaceutical Physical Chemistry, Graduate School of Medicine, Dentistry and Pharmaceutical Sciences, Okayama University, 1-1-1 Tsushima-naka, Okayama 700-8530, Japan*

[c] *Department of Pharmaceutical Health Chemistry, Faculty of Pharmaceutical Sciences, Matsuyama University, 4-2 Bunkyo-cho, Matsuyama 790-8578, Japan*

[d] *Department of Hygienic Chemistry, Faculty of Pharmaceutical Sciences, Fukuoka University, 8-19-1 Nanakuma, Minami-ku, Fukuoka 814-0180, Japan*

[e] *Developmental Research Laboratories, Shionogi & Co., Ltd., 3-1-1 Futaba-cho, Toyonaka 561-0825, Japan*

[f] *Department of Pharmacology, Graduate School of Medical and Dental Sciences, Kagoshima University, 8-35-1 Sakuragaoka, Kagoshima 890-8544, Japan*

ARTICLE INFO

*Article history:*
Received 2 June 2006
Accepted 25 August 2006

*Keywords:*
Marmoset
CYP2C8
Yeast cell
Tolbutamide
Quercetin

*Abbreviations:*
CYP, cytochrome P450
TB, tolbutamide
PT, paclitaxel
DF, diclofenac
S-MP, S-mephenytoin
G-6-P, glucose 6-phosphate

ABSTRACT

We cloned a cDNA encoding a novel CYP2C enzyme, called P450 M-2C, from a marmoset liver. The deduced amino acid sequence showed high identities to those of human CYP2C8 (87%), CYP2C9 (78%) and CYP2C19 (77%). The P450 M-2C enzyme expressed in yeast cells catalyzed *p*-methylhydroxylation of only tolbutamide among four substrates tested, paclitaxel as a CYP2C8 substrate, diclofenac and tolbutamide as CYP2C9 substrates and S-mephenytoin as a CYP2C19 substrate. *p*-Methylhydroxylation of tolbutamide by marmoset liver microsomes showed monophasic kinetics, and the apparent $K_m$ value (1.2 mM) for the substrate was similar to that of the recombinant P450 M-2C (1.8 mM). Although all of the recombinant human CYP2C8, CYP2C9 and CYP2C19 expressed in yeast cells catalyzed tolbutamide *p*-methylhydroxylation, the kinetic profile of CYP2C8 was most similar to that of P450 M-2C. Tolbutamide oxidation by the marmoset liver microsomes and the recombinant P450 M-2C was inhibited most effectively by quercetin, a CYP2C8 inhibitor, followed by omeprazole, a CYP2C19 inhibitor, whereas sulfaphenazole, a CYP2C9 inhibitor, was less potent under the conditions used. These results indicate that P450 M-2C is the major tolbutamide *p*-methylhydroxylase in the marmoset liver.



* *Corresponding author.* Tel.: +81 86 251 7942; fax: +81 86 251 7942.
E-mail address: shizuo@pharm.okayama-u.ac.jp (S. Narimatsu).

0006-2952/$ – see front matter © 2006 Elsevier Inc. All rights reserved.
doi:10.1016/j.bcp.2006.08.025

## 1. Introduction

Several kinds of monkeys such as rhesus monkeys, crab-eating monkeys, Japanese monkeys and marmoset monkeys, have been employed as one of experimental animals in research on drug metabolism and toxicity. The old-world monkeys, including rhesus monkeys, crab-eating monkeys and Japanese monkeys ranging through Africa, Europe and Asia, have disadvantages such as body sizes too big for easy handling and poor fertility. In contrast, marmoset monkeys, belonging to the new-world monkeys ranging through Central and South America are thought to be promising candidates for experimental animals, because of their small size, easy handling and breeding.

Cytochrome P450 (CYP) is a key enzyme for oxidative drug metabolism in mammals including humans and monkeys. CYP constitutes a superfamily and four CYP subfamilies, namely, CYP1, –2, –3 and –4, are mainly responsible for drug metabolism in humans [1–3]. Although CYP enzymes have been extensively characterized in humans and the old-world monkeys, relatively little information is available about the properties of CYP enzymes in marmoset monkeys.

Previous studies provided experimental evidence supporting the notion that pretreatment with chemical compounds such as phenobarbital [4], 3-methylcholanthrene, polychlorinated biphenyl [5], 2,3,7,8-tetrachlorodibenzo-*p*-dioxin [6,7] or isoniazide [8] induced CYP isoenzymes in marmosets. Using targeted anti-peptide antibodies, Schulz et al. [9] suggested the possible expression of CYP1A1, CYP1A2, CYP2A, CYP2B, CYP2C, CYP2E1 and CYP3A21 enzymes in marmosets. Moreover, the research group of Kamataki isolated cDNA clones encoding CYP1A2 [5], CYP2D19 and CYP3A21 [10] from marmoset livers, and characterized the enzymatic properties of CYP1A2 expressed in high-red yeast cells [5]. Recently, we also cloned cDNAs encoding CYP1A2 [11], CYP2D19 and CYP2D30 [12] from fresh marmoset livers, and expressed the proteins in yeast cells to examine their enzymatic functions. However, for prompt utilization of marmoset monkeys as experimental animals in the study of drug metabolism and toxicity, functional characterization of other drug-metabolzing enzymes in this species would be required. In the present study, we have cloned a cDNA encoding a novel CYP2C enzyme from marmoset liver, expressed the protein in yeast cells, and characterized its enzymatic functions.

## 2. Materials and methods

### 2.1. Materials

Peclitaxel (PT), tolbutamide (TB), quercetin, sulfaphenazole and omeprazole were purchased from Sigma Chemical Co. (St. Louis, MO); 6α-hydroxypaclitaxel was from Calbiochem (San Diego, CA), docetaxel trihydrate was from Toronto Research Chemicals Inc. (North York, Ontario, Canada); diclofenac (DF), N-phenylanthranilic acid, glucose 6-phosphate (G-6-P) dehydrogenase (from yeast) and NADPH were from Wako Pure Chemicals Co. (Osaka, Japan); 4′-hydroxydiclofenac, S-mephenytoin (S-MP) and 4′-hydroxymephenytoin were from Daiichi Chemical Co. (Tokyo, Japan); phenobarbital and chlorpropamide were from Tokyo Kasei Kogyo Co. (Tokyo, Japan). *p*-Methylhydroxytolbutamide was supplied from Dr. Takahiko Baba. Pooled human liver microsomes from donors (12 Caucasians and 1 Hispanic, 13 males, 4–62 years old; 9 females, 40–74 years old) were purchased from BD Biosciences Discovery Labware (Bedford, MA). Other chemical reagents or solvents used were of the highest quality commercially available.

### 2.2. Cloning of cDNA encoding a marmoset CYP2C enzyme

Total RNA was extracted from an adult female marmoset liver (2 years old, supplied from Kagoshima University) using an RNeasy mini kit (Qiagen, Hilden, Germany), and first-strand DNA was synthesized using an RNA PCR kit (Version 3.0, Takara Bio, Ohtsu, Japan) according to the manufacturer's instructions. A full length cDNA encoding a marmoset CYP enzyme was amplified by polymerase chain reaction (PCR) using the forward primer 5′-GTAAGAAGAGAAGTCTTCAATG-3′ and the reverse primer 5′-ATACAAGTGTTACCGAGTATGA-3′. These primers were designed based on the nucleotide sequence in the flanking regions of the crab-eating monkey CYP2C20 cDNA (GenBank accession no. S53046). The reaction mixtures (50 μl) contained 0.2 mM dNTPs, 1 mM $MgSO_4$, 1 U of KOD-plus DNA polymerase (Toyobo, Osaka, Japan) and each oligonucleotide primer at 0.5 μM. PCR consisted of 35 cycles of denaturation at 94 °C for 30 s, annealing at 50 °C for 30 s and extension at 68 °C for 100 s. The initial denaturation was performed at 94 °C for 120 s. The amplified product (1.5 kbp) was purified with a MinElute gel extraction kit (Qiagen), and the 5′- and 3′-ends of the coding region were sequenced in both the forward and reverse directions using ABI BigDye terminator cycle sequencing reaction kit v3.1 (Applied Biosystems, Piscaway, NJ).

The full-length cDNA thus obtained was modified by PCR amplification with 5′-AAGCTTAAAAAAATGGATCCTTTTGT-GGTCC-3′ and 5′-AAGCTTTCAGACAGGAATGAAGCAGATC-TG-3′ as primers under the conditions described above. *Hin*dIII sites (marked with solid lines) were introduced to the 5′-end of the start codon and the 3′-end of the stop codon to facilitate subcloning into the yeast expression vector (pGYR1). A Kozak sequence (marked in italics) was also introduced just upstream of the start codon to achieve high expression of the protein in yeast cells. The PCR products were ligated into pGEM-T (Promega, Madison, WI) using the TA cloning system, and the insert was sequenced in both the forward and reverse directions. The DNA fragment encoding a marmoset CYP2C (tentatively called P450 M-2C) was cut out with *Hin*dIII from the cloned pGEM-T and was subsequently subcloned into pGYR1 digested with the same enzyme. The insert of the plasmid was sequenced to verify the correct orientation with respect to the promoter for pGYR1. Construction of the expression plasmids containing each of CYP2C8, CYP2C9 and CYP2C19 cDNAs was described previously [13].

### 2.3. Expression of CYP2C enzymes

*Saccharomyces cerevisiae* AH22 was transformed with pGYR1 containing each of CYP cDNAs by the lithium acetate method, and the cultivation of yeast transformants thus obtained was performed as described [14]. A microsomal fraction was

prepared from yeast cells by the method previously reported [15].

### 2.4. Assays of M-2C holo- and apoproteins

The microsomal fraction prepared as above was diluted to a protein concentration of 10 mg/ml with 100 mM potassium phosphate buffer (pH 7.4) containing 20% (v/v) glycerol, and the total holo-CYP content was measured spectrophotometrically according to the method of Omura and Sato [16] using 91 $mM^{-1}$ $cm^{-1}$ as the absorption coefficient.

Marmoset liver microsomes were also prepared according to a published method [17]. Appropriate portions of the microsomal fractions of yeast cells, marmoset livers and pooled human livers were subjected to sodium dodecyl sulfate-polyacrylamide gel electrophoresis using a 10% slab gel. Following the electrophosresis, proteins on the gel were electroblotted to a polyvinylidene fluoride membrane, and were analyzed by Western blotting according to the method of Guengerich et al. [18] using rabbit anti-human CYP2C19 polyclonal antibody as a primary antibody (Daiichi Chemical Co.) and peroxidase-goat-anti-rabbit IgG (H + L) as a secondary antibody (Daiichi Chemical Co.).

### 2.5. Enzyme assay

PT 6α-hydroxylase activity in microsomal fractions from yeast cells expressing P450 M-2C or CYP2C8 was determined by the method of Soyama et al. [19] with a slight modification. Briefly, an ice-cold reaction mixture (500 μl) in a conical glass tube (10 ml) with a stopper contained 5 mM G-6-P, 1 IU of G-6-P dehydrogenase, 5 mM $MgCl_2$, 0.1 mM EDTA, 0.5 mM NADPH and PT (2.5, 5 and 10 μM). After preincubation at 37 °C for 5 min, the reaction was started by adding the microsomal fraction (20 pmol CYP) and was performed at 37 °C for 10 min. After the reaction was stopped by adding 3 ml of ethyl acetate and vortex mixing, 10 nmol of docetaxel was added as an internal standard, and the mixture was shaken at room temperature for 10 min. The mixture was then centrifuged at 1200 × *g* for 15 min, and 2 ml of the organic layer was taken, and evaporated *in vacuo*. The residue was dissolved in 200 μl of methanol/water (1:1, v/v), and an aliquot (10 μl) was subjected to HPLC under the conditions described below.

DF 4′-hydroxylase activity in microsomal fractions from yeast cells expressing M-2C or CYP2C9 was determined by the method of Schmitz et al. [20] with a slight modification. Briefly, a reaction mixture containing the same components described above except for the substrate (5, 20 or 100 μM DF instead of PT) was preincubated at 37 °C for 5 min, and the reaction was started by adding the microsomal fraction (20 pmol CYP) and was stopped 5 min later by adding 20 μl of 2 M phosphoric acid and vortexing. Then, 3 ml of t-butylmethylether and 0.8 nmol of N-phenylanthranilic acid as an internal standard were added, shaken vigorously, and centrifuged at 1200 × *g* for 15 min. The organic layer (2 ml) was taken, and evaporated *in vacuo*, and the residue was dissolved in 200 μl of methanol/water (1:1, v/v). An aliquot (10 μl) was subjected to HPLC under the conditions described below.

TB *p*-methylhydroxylase activities in microsomal fractions from yeast cells expressing P450 M-2C, CYP2C8, CYP2C9 or CYP2C19 and in pooled human liver microsomes were determined by the method of Komatsu et al. [21] with a slight modification. Briefly, a reaction mixture containing the same components described for PT 6α-hydroxylation except for the substrate (0.25, 1 or 2.5 μM TB instead of PT) was preincubated at 37 °C for 5 min, and the reaction was started by adding the microsomal fraction (20 pmol of recombinant CYP or 1 mg of human liver microsomes) and was stopped 10 min later for the recombinant enzymes and 40 min later for the human liver microsomes by adding 3 ml of ethyl acetate and vortexing. Then, 1.5 μg of chlorpropamide was added as an internal standard, and the mixture was shaken vigorously, and centrifuged at 1200 × *g* for 15 min. The organic layer (2 ml) was taken, and evaporated *in vacuo*, and the residue was dissolved in 200 μl of methanol/water (1:1, v/v). An aliquot (10 μl) was subjected to HPLC under the conditions described below.

S-MP 4′-hydroxylase activity in microsomal fractions from yeast cells expressing P450 M-2C or CYP2C19 was determined by the method of Nakajima et al. [22] with a slight modification. Briefly, a reaction mixture containing the same components described for PT 6α-hydroxylation except for the substrate (10, 50 or 200 μM S-MP instead of PT) was preincubated at 37 °C for 5 min, and the reaction was started by adding the microsomal fraction (20 pmol CYP) and was stopped 5 min later by adding 3 ml of dichloromethane and vortexing. Then 4 nmol of phenobarbital was added as an internal standard, and the mixture was shaken vigorously, and centrifuged at 1200 × *g* for 15 min. The organic layer (2 ml) was taken, and evaporated *in vacuo*, and the residue was dissolved in 200 μl of $CH_3OH$/water (1:1, v/v). An aliquot (10 μl) was subjected to HPLC under the conditions described below.

The HPLC conditions were: a Hitachi 655A-12 liquid chromatograph equipped with an L-5000 LC controller, a 655A variable wavelength UV monitor, a Rheodyne model 7125 injector and a Shimadzu C-R3A Chromatopac data processor; column, Inertsil ODS 80A (4.6 mm × 150 mm, GL Science Co., Tokyo, Japan) at 40 °C; mobile phase, water/$CH_3CN$/$CH_3OH$ (52:34:14, v/v) at a flow rate of 1.2 ml/min for PT 6α-hydroxylation (detection, 230 nm), 30 mM potassium phosphate buffer (pH 6.5)/$CH_3CN$/$CH_3OH$ (64:16:20, v/v) at a flow rate of 1.2 ml/min for DF 4′-hydroxylation (detection, 280 nm), 20 mM potassium phosphate buffer (pH 4)/$CH_3CN$/$CH_3OH$ (77:6:17, v/v) at a flow rate of 1.0 ml/min for S-MP 4′-hydroxylation (detection, 204 nm), and 0.05% phosphoric acid/$CH_3CN$ (72:28, v/v) at a flow rate of 1.0 ml/min for TB *p*-methylhydroxylation (detection, 230 nm). For each enzyme assay, calibration curves were made by adding various amounts of synthetic metabolites to ice-cold reaction mixtures containing the same components described above. Intra- and inter-day variation coefficients did not exceed 10% in any assay.

### 2.6. Kinetic and inhibition studies

Kinetic studies for TB *p*-methylhydroxylation were performed using substrate concentration ranges of 0.1–10 mM for P450 M-2C, 0.1–7.5 mM for CYP2C8, 0.025–2.5 mM for CYP2C9 and human liver microsomes, 0.05–5 mM for CYP2C19, and 0.01–5 mM for marmoset liver microsomes. Apparent Michaelis–Menten constants ($K_m$) and maximal velocities ($V_{max}$) were

```
   1  ATG GAT CCT TTT GTG GTC CTG TTG CTC TGT CTC TCT TTT TTG CTT CTC TTT TCA CTC TGG  60
   1  Met Asp Pro Phe Val Val Leu Leu Leu Cys Leu Ser Phe Leu Leu Leu Phe Ser Leu Trp  20

  61  AGA CAG AGC TCT GGG AGA GGG AAG CTC CCT CCT GGC CCC ACT CCT CTT CCT ATT ATT GGA  120
  21  Arg Gln Ser Ser Gly Arg Gly Lys Leu Pro Pro Gly Pro Thr Pro Leu Pro Ile Ile Gly  40

 121  AAC ATC CTA CAG ATA AGT GTT AAG GAC ATC GGC AAA TCT TTC AGC AAT CTC TCA AAA GTC  180
  41  Asn Ile Leu Gln Ile Ser Val Lys Asp Ile Gly Lys Ser Phe Ser Asn Leu Ser Lys Val  60

 181  TAT GGT CCT CTG TTC ACC GTG TAT TTT GGC ACG AAG CCC GTA GTG GTG TTG CAC GGA TAT  240
  61  Tyr Gly Pro Leu Phe Thr Val Tyr Phe Gly Thr Lys Pro Val Val Val Leu His Gly Tyr  80

 241  GAG GCA GTA AAG GAA GCC CTG ATT GAT AAT GGA GAG GAG TTT TCT GGA AGA AGC ATT TTC  300
  81  Glu Ala Val Lys Glu Ala Leu Ile Asp Asn Gly Glu Glu Phe Ser Gly Arg Ser Ile Phe  100

 301  CCA GTA TCT CAA AGA ACT TCT AAA GAT CTT GGA ATC ATT TCC AGC AAT GGA AAG AGA TGG  360
 101  Pro Val Ser Gln Arg Thr Ser Lys Asp Leu Gly Ile Ile Ser Ser Asn Gly Lys Arg Trp  120

 361  AAG GAG ATC CGG CGT TTC TCC CTT ACA ACA TTG CGG AAT TTT GGG ATG GGG AAG AGG AGC  420
 121  Lys Glu Ile Arg Arg Phe Ser Leu Thr Thr Leu Arg Asn Phe Gly Met Gly Lys Arg Ser  140

 421  ATT GAG GAC CGT GTT CAA CAA GAA GCC CGC TGC CTT GTG GAG GAG TTG AGA AAA ACC AAG  480
 141  Ile Glu Asp Arg Val Gln Gln Glu Ala Arg Cys Leu Val Glu Glu Leu Arg Lys Thr Lys  160

 481  GCC TCA CCC TGT GAT CCC ACT TTC ATC CTG GGC TGT GCT CCC TGC AAT GTG ATC TGC TCC  540
 161  Ala Ser Pro Cys Asp Pro Thr Phe Ile Leu Gly Cys Ala Pro Cys Asn Val Ile Cys Ser  180

 541  GTT GTT TTC CAG AAT CGA TTT GAT TAT AAA GAT GAA AAT TTT CTC ACC CTG ATG AAA AGG  600
 181  Val Val Phe Gln Asn Arg Phe Asp Tyr Lys Asp Glu Asn Phe Leu Thr Leu Met Lys Arg  200

 601  TTC AAT GAA AAC TTC AAG ATT CTG AGC TCT CCA TGG ATC CAG TTC TGC AAT AAT TTC CCT  660
 201  Phe Asn Glu Asn Phe Lys Ile Leu Ser Ser Pro Trp Ile Gln Phe Cys Asn Asn Phe Pro  220

 661  CTC CTC ATG GAT TAT TTC CCA GGA CCT CAC AAC AAA TTG TTT AAA AAT GTT GCT CTT ACA  720
 221  Leu Leu Met Asp Tyr Phe Pro Gly Pro His Asn Lys Leu Phe Lys Asn Val Ala Leu Thr  240

 721  AAA AGC TAT ATT TGG GAG AAA ATA AAA GAA CAC CAA GCA TCA CTG GAT GTT AAC AAT CCT  780
 241  Lys Ser Tyr Ile Trp Glu Lys Ile Lys Glu His Gln Ala Ser Leu Asp Val Asn Asn Pro  260

 781  CGG GAC TTT ATC GAT TGC TTT CTG ATC AAA ATG CAG CAG GAA AAG GAC AAC CAA GAG TCT  840
 261  Arg Asp Phe Ile Asp Cys Phe Leu Ile Lys Met Gln Gln Glu Lys Asp Asn Gln Glu Ser  280

 841  GAA TTC ACT ATT GAA AGC TTG GTT GGC ACT GTA GCT GAT CTA TTT GTT GCT GGA ACA GAG  900
 281  Glu Phe Thr Ile Glu Ser Leu Val Gly Thr Val Ala Asp Leu Phe Val Ala Gly Thr Glu  300

 901  ACA ACA AGC ACC ACT CTG AGA TAT GGA CTC CTA CTC CTG CTG AAG CAC CCA GAG GTC ACA  960
 301  Thr Thr Ser Thr Thr Leu Arg Tyr Gly Leu Leu Leu Leu Leu Lys His Pro Glu Val Thr  320

 961  GCT AAA GTC CAG GAA GAG ATT GAT CAT GTA ATT GGC AGA CAC AGG AGC CCC TGC ATG CAG  1020
 321  Ala Lys Val Gln Glu Glu Ile Asp His Val Ile Gly Arg His Arg Ser Pro Cys Met Gln  340

1021  GAT AGG AGC CAC ATG CCT TAT ACA GAT GCT GTC ATG CAC GAG ATC CAG AGA TAC ATT GAC  1080
 341  Asp Arg Ser His Met Pro Tyr Thr Asp Ala Val Met His Glu Ile Gln Arg Tyr Ile Asp  360

1081  CTT GTC CCC ACC AGT GTG CCC CAT GCA GTG ACC ACT GAC ATT AAG TTC AGA AAT TAC CTC  1140
 361  Leu Val Pro Thr Ser Val Pro His Ala Val Thr Thr Asp Ile Lys Phe Arg Asn Tyr Leu  380

1141  ATC CCC AAG GGC ACA GCC ATA ATG ACA TCA CTG ACT TCA GTG CTG CAC AGT GAC AAA GAA  1200
 381  Ile Pro Lys Gly Thr Ala Ile Met Thr Ser Leu Thr Ser Val Leu His Ser Asp Lys Glu  400

1201  TTT CCC AAT CCA AAG ACC TTT GAC CCT GGC CAC TTT CTG GAT AAA AAT GGC AAC TTT AAG  1260
 401  Phe Pro Asn Pro Lys Thr Phe Asp Pro Gly His Phe Leu Asp Lys Asn Gly Asn Phe Lys  420

1261  AAA AGT GAC CAC TTC ATG CCT TTC TCA GCA GGG AAA CGA ATT TGT GCT GGA GAG GGA CTC  1320
 421  Lys Ser Asp His Phe Met Pro Phe Ser Ala Gly Lys Arg Ile Cys Ala Gly Glu Gly Leu  440

1321  GCC CGC ATG GAG ATA TTT TTA TTC CTA ACC ACA ATT TTA CAG AAC TTT AAT CTG AAA TCT  1380
 441  Ala Arg Met Glu Ile Phe Leu Phe Leu Thr Thr Ile Leu Gln Asn Phe Asn Leu Lys Ser  460

1381  GTT GGC GAT ATA AAG AAC CTC AAT ACT ACT TCA GCT AGC AAA TCA ATT GTT TCT TTG CCA  1440
 461  Val Gly Asp Ile Lys Asn Leu Asn Thr Thr Ser Ala Ser Lys Ser Ile Val Ser Leu Pro  480

1441  CCC CCG TAC CAG ATC TGC TTC ATT CCT GTC TGA  1473
 481  Pro Pro Tyr Gln Ile Cys Phe Ile Pro Val End
```

**Fig. 1 – Nucleotide and deduced amino acid sequences of marmoset P450 M-2C. The numbers of the amino acids and nucleotides are shown in upper and lower lines, respectively.**

```
M-2C        1  MDPFVVLLLCLSFLLLFSLWRQSSGRGKLPPGPTPLPIIGNILQISVKDIGKSFSNLSKV  60
CYP2C8      1  MEPFVVLVLCLSFMLLFSLWRQSCRRRKLPPGPTPLPIIGNMLQIDVKDICKSFTNFSKV  60
CYP2C9      1  MDSLVVLVLCLSCLLLLSLWRQSSGRGKLPPGPTPLPVIGNILQIGIKDISKSLTNLSKV  60
CYP2C19    61  MDPFVVLVLCLSCLLLLSIWRQSSGRGKLPPGPTPLPVIGNILQIDIKDVSKSLTNLSKI  60
               *   *** ****  ** * ****  * ********** *** ***  **  **  * **

                                                          SRS-1
M-2C       61  YGPLFTVYFGTKPVVVLHGYEAVKEALIDNGEEFSGRSIFPVSQRTSKDLGIISSNGKRW  120
CYP2C8     61  YGPVFTVYFGMNPIVVFHGYEAVKEALIDNGEEFSGRGNSPISQRITKGLGIISSNGKRW  120
CYP2C9     61  YGPVFTLYFGLKPIVVLHGYEAVKEALIDLGEEFSGRGIFPLAERANRGFGIVFSNGKKW  120
CYP2C19    61  YGPVFTLYFGLERMVVLHGYEVVKEALIDLGEEFSGRGHFPLAERANRGFGIVFSNGKRW  120
               *** ** ***    ** **** ******* *******   *   *     **  **** *

M-2C      121  KEIRRFSLTTLRNFGMGKRSIEDRVQQEARCLVEELRKTKASPCDPTFILGCAPCNVICS  180
CYP2C8    121  KEIRRFSLTNLRNFGMGKRSIEDRVQEEAHCLVEELRKTKASPCDPTFILGCAPCNVICS  180
CYP2C9    121  KEIRRFSLMTLRNFGMGKRSIEDRVQEEARCLVEELRKTKASPCDPTFILGCAPCNVICS  180
CYP2C19   121  KEIRRFSLMTLRNFGMGKRSIEDRVQEEARCLVEELRKTKASPCDPTFILGCAPCNVICS  180
               ********  ***************** ** ******************************

                          SRS-2                                  SRS-3
M-2C      181  VVFQNRFDYKDENFLTLMKRFNENFKILSSPWIQFCNNFPLLMDYFPGPHNKLFKNVALT  240
CYP2C8    181  VVFQKRFDYKDQNFLTLMKRFNENFRILNSPWIQVCNNFPLLIDCFPGTHNKVLKNVALT  240
CYP2C9    181  IIFHKRFDYKDQQFLNLMEKLNENIKILSSPWIQICNNFSPIIDYFPGTHNKLLKNVAFM  240
CYP2C19   181  IIFQKRFDYKDQQFLNLMEKLNENIRIVSTPWIQICNNFPTIIDYFPGTHNKLLKNLAFM  240
                 *  ******  ** **   ***  *   **** ****    * *** ***  ** *

                                                          SRS-4
M-2C      241  KSYIWEKIKEHQASLDVNNPRDFIDCFLIKMQQEKDNQESEFTIESLVGTVADLFVAGTE  300
CYP2C8    241  RSYIREKVKEHQASLDVNNPRDFMDCFLIKMEQEKDNQKSEFNIENLVGTVADLFVAGTE  300
CYP2C9    241  KSYILEKVKEHQESMDMNNPQDFIDCFLMKMEKEKHNQPSEFTIESLENTAVDLFGAGTE  300
CYP2C19   241  ESDILEKVKEHQESMDINNPRDFIDCFLIKMEKEKQNQQSEFTIENLVITAADLLGAGTE  300
               * * ** **** * * *** ** **** **  ** ** *** ** *  *  **  ****

          ____                                                        ___
M-2C      301  TTSTTLRYGLLLLLKHPEVTAKVQEEIDHVIGRHRSPCMQDRSHMPYTDAVMHEIQRYID  360
CYP2C8    301  TTSTTLRYGLLLLLKHPEVTAKVQEEIDHVIGRHRSPCMQDRSHMPYTDAVVHEIQRYSD  360
CYP2C9    301  TTSTTLRYALLLLLKHPEVTAKVQEEIERVIGRNRSPCMQDRSHMPYTDAVVHEVQRYID  360
CYP2C19   301  TTSTTLRYALLLLLKHPEVTAKVQEEIERVIGRNRSPCMQDRGHMPYTDAVVHEVQRYID  360
               ******** ******************  **** ******** ******** ** *** *
               SRS-5
M-2C      361  LVPTSVPHAVTTDIKFRNYLIPKGTAIMTSLTSVLHSDKEFPNPKTFDPGHFLDKNGNFK  420
CYP2C8    361  LVPTGVPHAVTTDTKFRNYLIPKGTTIMALLTSVLHDDKEFPNPNIFDPGHFLDKNGNFK  420
CYP2C9    361  LLPTSLPHAVTCDIKFRNYLIPKGTTILISLTSVLHDNKEFPNPEMFDPHHFLDEGGNFK  420
CYP2C19   361  LIPTSLPHAVTCDVKFRNYLIPKGTTILTSLTSVLHDNKEFPNPEMFDPRHFLDEGGNFK  420
               * **  ***** * ********** *   ******  ******  *** ****  ****

                                                          SRS-6
M-2C      421  KSDHFMPFSAGKRICAGEGLARMEIFLFLTTILQNFNLKSVGDIKNLNTTSASKSIVSLP  480
CYP2C8    421  KSDYFMPFSAGKRICAGEGLARMELFLFLTTILQNFNLKSVDDLKNLNTTAVTKGIVSLP  480
CYP2C9    421  KSKYFMPFSAGKRICVGEALAGMELFLFLTSILQNFNLKSLVDPKNLDTTPVVNGFASVP  480
CYP2C19   421  KSNYFMPFSAGKRICVGEGLARMELFLFLTFILQNFNLKSLIDPKDLDTTPVVNGFASVP  480
               **  ********** ** ** ** ***** *********  * * * **       * *

M-2C      481  PPYQICFIPV  491
CYP2C8    481  PSYQICFIPV  491
CYP2C9    481  PFYQLCFIPV  491
CYP2C19   481  PFYQLCFIPV  491
               * ** *****
```

**Fig. 2 – Multiple alignment of the amino acid sequences of P450 M-2C, human CYP2C8, CYP2C9 and CYP2C19. *Amino acid residues conserved among the four CYP2C enzymes. Six substrate recognition sites (SRSs) are shown with lines.**

analyzed on the basis of Michaelis–Menten plots or Eadie–Hofstee plots using Prism Version 4 (Graphpad Software, San Diego, CA). Inhibition experiments using quercetin (10, 50 and 200 μM), sulfaphenazole (20, 50 and 200 μM) and omeprazole (50, 200 and 500 μM) and substrate (TB) concentrations of 0.1 and 1 mM were performed for marmoset liver microsomes and yeast cell microsomes expressing P450 M-2C. Each inhibitor was dissolved in a mixture of methanol/dimethylsulfoxide (1:1, v/v) and the final concentration of the organic solvent in the reaction mixture was less than 1%. Control experiments were run with the vehicle only instead of the inhibitors. $IC_{50}$ values were analyzed using Prism. Protein concentrations were measured by the method of Lowry et al. [23] using bovine plasma albumin as a standard.

### 2.7. *Molecular modeling*

The homology model of P450 M-2C was constructed by Swiss-Model (http://swissmodel.expasy.org/) using the crystallo-

Table 1 – Identities of the nucleotide and deduced amino acid sequences of eight CYP2C enzymes in primates

| | M-2C | CYP2C8 | CYP2C9 | CYP2C19 | CYP2C20 | CYP2C43 | CYP2C74 | CYP2C75 |
|---|---|---|---|---|---|---|---|---|
| M-2C | | 92.7 | 84.5 | 83.8 | 93.1 | 83.3 | 93.1 | 83.6 |
| CYP2C8 | 87.1 | | 84.7 | 84.9 | 95.6 | 83.8 | 95.5 | 84.5 |
| CYP2C9 | 78.4 | 77.6 | | 94.8 | 84.5 | 95.2 | 84.5 | 95.9 |
| CYP2C19 | 77.1 | 77.8 | 91.4 | | 84.7 | 93.8 | 84.6 | 94.8 |
| CYP2C20 | 88.8 | 91.6 | 78.2 | 78.6 | | 83.2 | 99.6 | 84.3 |
| CYP2C43 | 76.7 | 77.1 | 92.2 | 90.0 | 77.1 | | 83.1 | 95.1 |
| CYP2C74 | 89.0 | 91.6 | 78.2 | 78.4 | 99.4 | 76.9 | | 84.2 |
| CYP2C75 | 76.5 | 76.7 | 93.9 | 92.0 | 77.1 | 93.5 | 76.9 | |

Upper-right values, percentage identities of the nucleotide sequences; lower-left values, percentage identities of deduced amino acid sequences.

graphic data of CYP2C8 (1PQ2) obtained from Protein Data Bank (http://www.rcsb.org/pdb/) and the primary amino acid sequence of P450 M-2C determined in this work. Hydrogen atoms were further added for the P450 M-2C homology model using the Biopolymer module of Insight II software package (Molecular Simulations Inc., San Diego, CA). Six peptides of P450 M-2C (Arg-97 to Asn-116, Met-198 to Ser-209, Phe-234 to Leu-239, Gly-289 to Ser-303, Ile-359 to His-368, and Thr-469 to Ser-478) were extracted as substrate recognition sites (SRSs). The active-site cavities of CYP2C8 and P450 M-2C were made manually above the sixth ligand of heme at 1.0 Å resolution using a homemade CG program working on Windows PC. The amino acid residues at the active sites of CYP2C8 and P450 M-2C were drawn using RasMol Version 2.6-ucb-1.0 as described elsewhere [24].

## 3. Results

### 3.1. *Sequence analysis*

As shown in Fig. 1, the cloned cDNA consisted of 1473 base pairs starting with an initiation codon ATG and ending with a termination codon TGA. Fig. 2 depicts a comparison of deduced amino acid sequences of P450 M-2C, human CYP2C8, CYP2C9 and CYP2C19. The nucleotide and amino acid sequences are compared with those of human and monkey P450s belonging to the CYP2C subfamily in Table 1. The nucleotide sequence of the cDNA encoding marmoset P450 M-2C showed 92.7, 84.5, 83.8, 93.1, 83.3, 93.1 and 83.6% identities to human CYP2C8 (GenBank accession no. NM-000770), CYP2C9 (NM-000771), CYP2C19 (NM-000769), crab-eating mon-

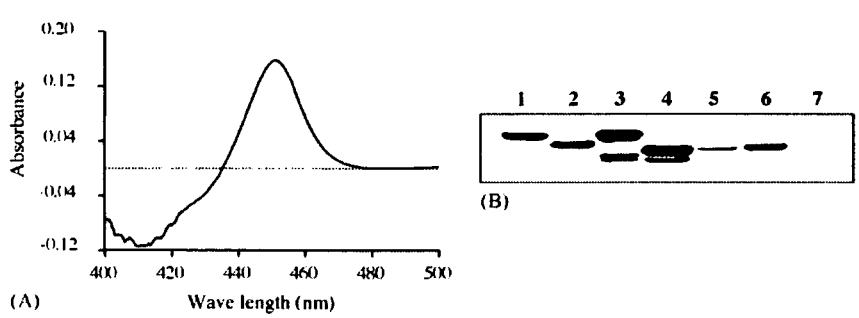


**Fig. 3 – A reduced CO-difference spectrum of yeast cell microsomes expressing marmoset P450 M-2C (A) and Western blot analysis of microsomal fractions from human and marmoset livers and of yeast cells expressing P450 M-2C and human CYP2C enzymes (B). (A) The protein concentration used was 10 mg/ml. (B) Lane 1, human liver microsomes; lane 2, yeast cell microsomes expressing human CYP2C8; lane 3, yeast cell microsomes expressing human CYP2C9; lane 4, yeast cell microsomes expressing human CYP2C19; lane 5, yeast cell microsomes expressing marmoset P450 M-2C; lane 6, marmoset liver microsomes; lane 7, mock. The amounts of microsomal proteins used were 30 μg for human and marmoset livers and 15 μg for yeast cells expressing P450 M-2C and human CYP2C enzymes.**

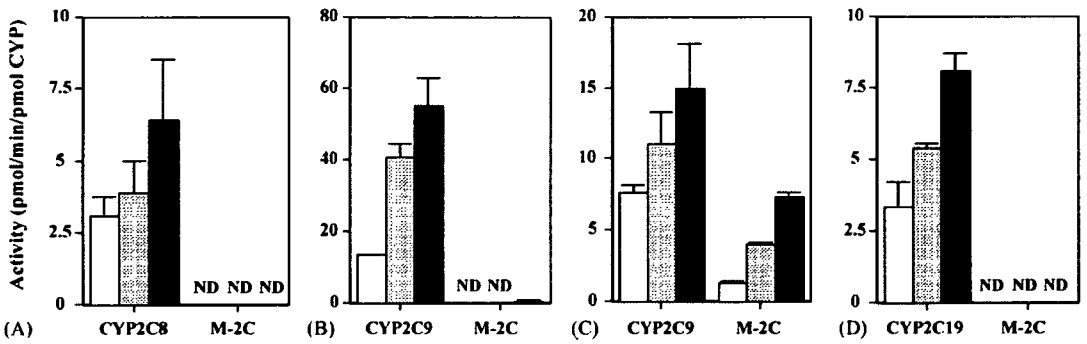


**Fig. 4 – Comparison of various drug oxidation activities between P450 M-2C and human CYP2C enzymes. (A) PT (2.5, 5 and 10 μM) 6α-hydroxylation, (B) DF (5, 20 and 100 μM) 4′-hydroxylation, (C) TB (0.25, 1 and 2.5 mM) p-methylhydroxylation and (D) S-MP (10, 50 and 200 μM) 4′-hydroxylation. Open, dotted and hatched columns show the lowest, intermediate and highest concentrations, respectively. Each value represents the mean ± S.D. of three independent determinations. ND, not detectable.**

key CYP2C20 (S53046), rhesus monkey CYP2C43 (AB212264), CYP2C74 (AY635462) and CYP2C75 (AY635463), respectively. The deduced amino acid sequence of P450 M-2C was highly identical to those of human CYP2C8 (87.1% identity), crab-eating monkey CYP2C20 (88.8%) and rhesus monkey CYP2C74 (89.0%).

### 3.2. *Expression of marmoset P450-M-2C protein in yeast cells*

The microsomal fraction was prepared from yeast cells expressing P450 M-2C, and the content of the recombinant holoenzyme was determined by reduced CO-difference spectroscopy (Fig. 3, left panel). The spectrum showed a Soret peak at 450 nm and a negligible level of peak at 420 nm. The content of P450 M-2C was calculated to be 133 pmol/mg protein (the mean value of two independent determinations). In Western blot analysis using polyclonal antibodies raised against human CYP2C19 (Fig. 3, right panel), microsomal fractions from yeast cells expressing P450 M-2C (lane no. 5) and from the marmoset liver (lane no. 6) exhibited a single protein band with a molecular weight similar to that of recombinant CYP2C19 (lane no. 4). In contrast, the pooled human liver microsomal fraction (lane no. 1) showed a major protein band whose molecular weight was similar to that of recombinant CYP2C9 (lane no. 3) and additional three faint protein bands, two of which exhibited similar mobilities to recombinant CYP2C8 (lane no. 2) and CYP2C19 (lane no. 4).

### 3.3. *Drug oxidation activities*

The recombinant P450 M-2C did not show any detectable oxidation activities towards PT or S-MP under the conditions used (Fig. 4A and D). A slight activity was observed for DF 4′-hydroxylation by P450 M-2C at the highest substrate concentration used (100 μM) (Fig. 4B). P450 M-2C exerted considerable TB p-methylhydroxylase activities, which were 20–50% those of CYP2C9 at substrate concentrations from 0.25 to 2.5 mM (Fig. 4C). Based on these results, we performed kinetic studies for TB p-methylhydroxylation by P450 M-2C and compared the results with those of human CYP2C8, CYP2C9 and CYP2C19.

TB p-methylhydroxylation by four recombinant CYP enzymes showed monophasic kinetics in Michaelis–Menten plots (data not shown). The kinetic parameters obtained are summarized in Table 2. The recombinant CYP enzymes could be divided into two groups, *i.e.*, high-$K_m$ group (P450 M-2C and CYP2C8) and low-$K_m$ group (CYP2C9 and CYP2C19).

TB p-methylhydroxylation by microsomal fractions from human and marmoset livers was analyzed by Eadie–Hofstee plots (data not shown). In human liver, microsomal TB

Table 2 – Kinetic parameters for TB p-methylhydroxylation by microsomal fractions from yeast cells expressing marmoset and human CYP enzymes and from human and marmoset livers

| Enzyme source | $K_m$ (μM) | $V_{max}$ | $V_{max}/K_m$ |
|---|---|---|---|
| Recombinant enzyme[a] | | | |
| P450 M-2C | 1780 | 11.8 | 0.0066 |
| CYP2C8 | 1520 | 2.5 | 0.0017 |
| CYP2C9 | 335 | 16.2 | 0.048 |
| CYP2C19 | 649 | 32.4 | 0.050 |
| Liver microsomal fraction[b] | | | |
| HLM | 318 ($K_{m1}$) | 185 ($V_{max1}$) | 0.582 ($V_{max1}/K_{m1}$) |
| | 72.7 ($K_{m2}$) | 246 ($V_{max2}$) | 3.38 ($V_{max2}/K_{m2}$) |
| MLM | 1170 | 470 | 0.402 |

[a] $V_{max}$, pmol/min/pmol CYP; $V_{max}/K_m$, μl/min/pmol CYP.
[b] $V_{max}$, pmol/min/mg protein; $V_{max}/K_m$, μl/min/mg protein. HLM, human liver microsomes; MLM, marmoset liver microsomes. Each value represents the mean of two independent determinations.

Table 3 – The $IC_{50}$ values for inhibitors of TB p-methylhydroxylation by mormoset liver microsomes and recombinant P450 M-2C

| Inhibitor | Marmoset liver microsomes | | Recombinant P450 M-2C | |
|---|---|---|---|---|
| | 0.1 mM[a] | 1 mM[a] | 1 mM[a] | 2 mM[a] |
| Quercetin | 51.4 | 16.1 | 105 | 61.2 |
| Sulfaphenazole | >200 | >200 | >200 | >200 |
| Omeprazole | 146 | 247 | 328 | 274 |

[a] Substrate concentration. $IC_{50}$ values are expressed as μM.

p-methylhydroxylation showing biphasic kinetics, the higher $K_m$ value ($K_{m1}$, 320 μM) was close to that of CYP2C9 (340 μM), while the lower $K_m$ value ($K_{m2}$, 70 μM) was much smaller than any $K_m$ values of the recombinant CYP enzymes examined (Table 2). This indicates that together with CYP2C9, another CYP enzyme having a lower $K_m$ value is also involved in TB p-methylhydroxylation by the pooled human liver microsomal fractions employed. On the other hand, in marmoset liver microsomal TB oxidation showing monophasic kinetics (data not shown), the $K_m$ value (1.2 mM) was close to that of P450 M-2C (1.8 mM) (Table 2), suggesting that P450 M-2C is the major TB p-methylhydroxylase in the mormoset liver.

### 3.4. Inhibition studies

The effects of three kinds of inhibitors, quercetin as a CYP2C8 inhibitor [25], sulfaphenazole as a CYP2C9 inhibitor [26] and omeprazole as a CYP2C19 inhibitor [27], on TB p-methylhydroxylation by microsomal fractions from mormoset liver (Fig. 5, upper panels) and yeast cells expressing P450 M-2C (Fig. 5, lower panels) were examined using two substrate concentrations of 0.1 and 1 mM. Quercetin (Fig. 5A and D) and omeprazole (Fig. 5C and F) similarly inhibited the TB oxidation activity of marmoset liver microsomes and recombinant P450 M-2C in a concentration-dependent manner. The potency of sulfaphenazole was lower than those of the other inhibitors (Fig. 5B and E). Table 3 lists the $IC_{50}$ values for the inhibitors. The potencies of the inhibitors were ranked as quercetin > omeprazole > sulfaphenazole for both marmoset liver microsomes and recombinant P450 M-2C.

## 4. Discussion

In the present study, we have cloned a cDNA encoding a novel CYP enzyme from the fresh liver of an adult female marmoset. The deduced amino acid sequence exhibited high identities to human CYP2C8 (87%), crab-eating monkey CYP2C20 (89%) and rhesus monkey CYP2C74 (89%). The nucleotide and amino acid sequences were registered to GenBank (accession no. AB242600). Dr. David Nelson, University of Tennessee Menphis, recommended us to call this CYP "marmoset CYP2C8" (his personal communication). In this paper, however, we tentatively called the enzyme P450 M-2C, standing for the Marmoset CYP2C enzyme to avoid confusion with human CYP2C8.

According to the list of P450 families and subfamilies of Dr. Nelson's home page (http://drnelson.utmem.edu/P450.stats.all.2005.htm), four monkey cDNA sequences encoding CYP2C enzymes had been registered as of January 8, 2005: crab-eating monkey CYP2C20 (S53046), rhesus monkey CYP2C43 (AB212264), CYP2C74 (AY635462) and CYP2C75 (AY635463). The functions of these monkey CYP enzymes have not been studied in detail, except for CYP2C43.

Matsunaga et al. [28] cloned a cDNA encoding CYP2C43 and characterized the enzymatic properties of CYP2C43 protein expressed in yeast cells. They reported that the recombinant CYP2C43 catalyzed S-MP 4′-hydroxylation but not TB p-methylhydroxylation under the conditions they employed. Interestingly, marmoset P450 M-2C showed the reverse substrate specificity, i.e., it catalyzed TB p-methylhydroxylation but not S-MP 4′-hydroxylation.

P450 M-2C showed considerable oxidation activity only for TB among the four substrates of human CYP2C enzymes examined. Although all of the human CYP2C enzymes (CYP2C8, CYP2C9 and CYP2C19) examined exerted TB oxidation activities, the kinetic profile of CYP2C8 was most similar to that of marmoset P450 M-2C (Table 2). The results of the inhibition study demonstrated that quercetin, a CYP2C8 inhibitor, was the most effective inhibitor for TB oxidation by P450 M-2C as well as by marmoset liver microsomes, followed by omeprazole, a CYP2C19 inhibitor. TB p-methylhydroxylation was kinetically

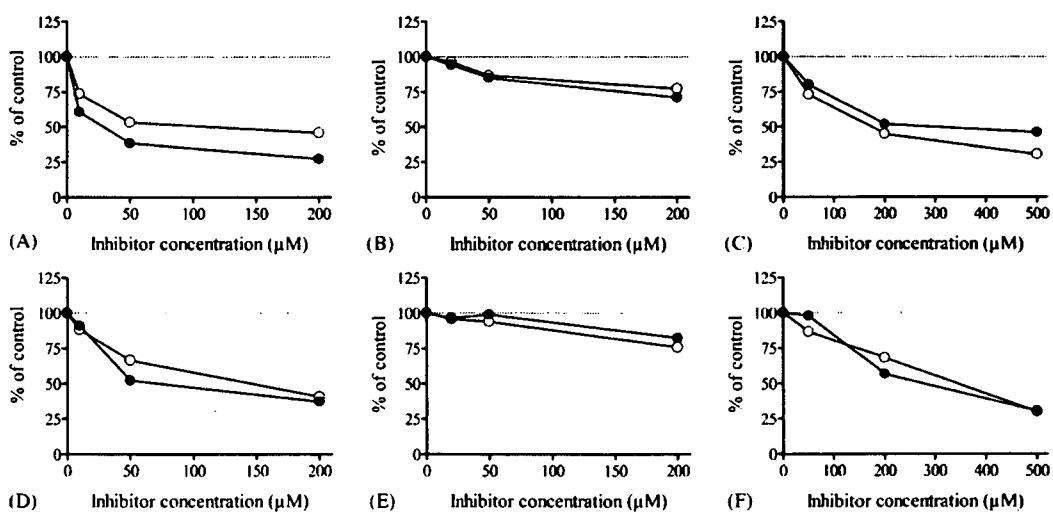


**Fig. 5 – The effects of human CYP2C enzyme inhibitors on TB p-methylhydroxylation by marmoset liver microsomes (upper panels) and by P450 M-2C (lower panels). The final inhibitor concentrations used were 10, 50 and 200 μM for quercetin (A and D) 20, 50 and 200 μM for sulfaphenazole (B and E) and 50, 200 and 500 μM for omeprazole (C and F). The substrate concentrations used were 100 (open circles) and 1000 μM (closed circles). Each point represents the mean of two independent determinations.**

analyzed to be monophasic, and the apparent $K_m$ values were similar between the marmoset liver microsomes and the recombinant P450 M-2C, indicating that P450 M-2C is the major TB p-methylhydroxylase in the marmoset liver.

It is well known that CYP2C9 is the major TB p-methylhydroxylase in the human liver [26]. However, TB p-methylhydroxylation gave biphasic kinetics in the pooled human liver microsomes used in the present study. The apparent $K_m$ value for TB p-methylhydroxylation by recombinant CYP2C9 was 340 μM in this study, which was close to the $K_m$ values of purified CYP2C9 reported by Lasker et al. [29] (180–400 μM) and of recombinant CYP2C9 (410 μM) reported by Flanagan et al. [30] for TB p-methylhydroxylation. Therefore, it is reasonable to think that some CYP enzyme(s) with a lower $K_m$ value of around 70 μM together with CYP2C9 with a higher $K_m$ value of 340 μM are responsible for TB p-methylhydroxylation in the human liver microsomal fractions used.

As described above, for TB p-methylhydroxylation, P450 M-2C and CYP2C8 showed similar kinetic profiles in the present study. In contrast, P450 M-2C did not show any detectable activity for PT 6α-hydroxylation, which was catalyzed by CYP2C8. Fig. 6 shows the active sites of P450 M-2C and CYP2C8. In a modeling study on PT 6α-hydroxylation by CYP2C8, Tanaka et al. [31] proposed that there are two distal sites (1 and 2) in addition to the proximal site occupying the space just above the heme iron in the active site of CYP2C8. They thought

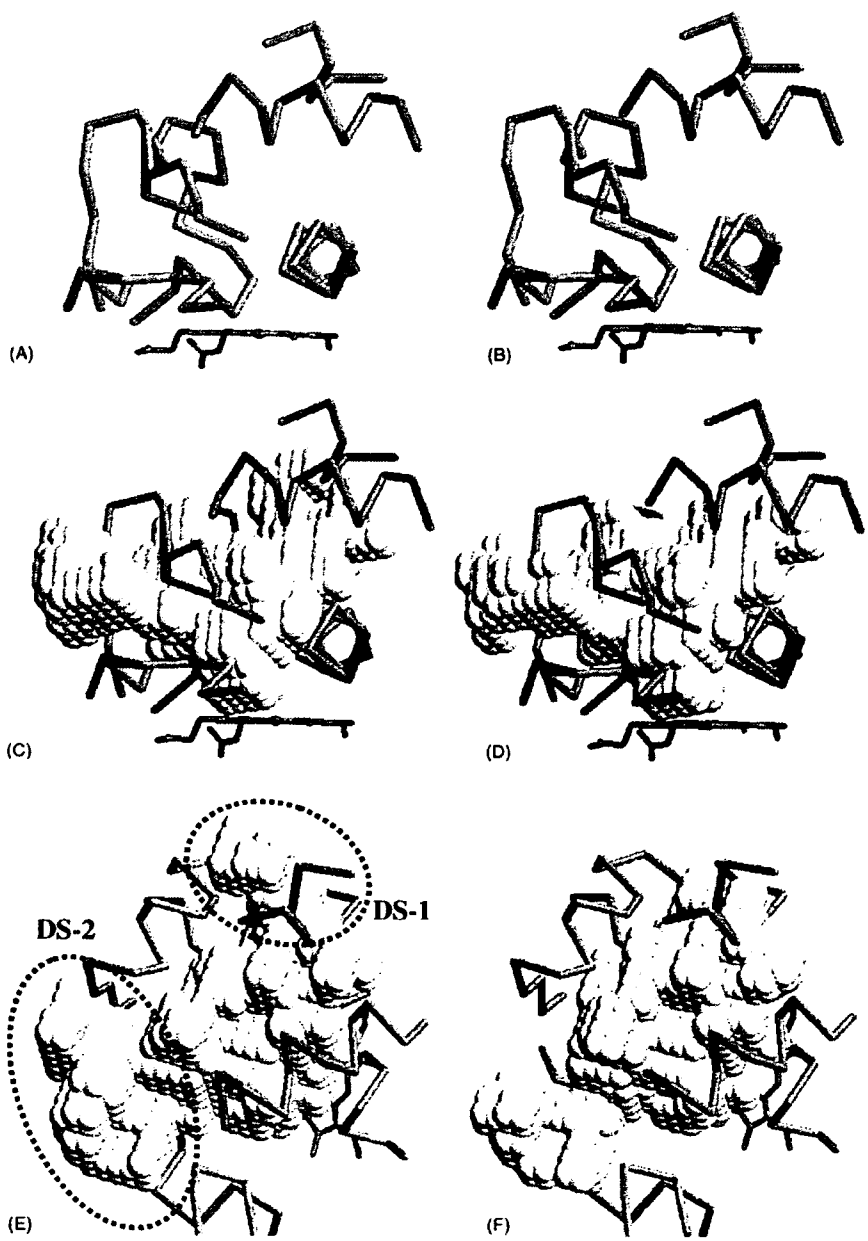


**Fig. 6 – Comparison of the active site structures (A and B) and the active site cavities (C–F) between CYP2C8 (left panels) and P450 M-2C (right panels). The active site conformation was depicted using RasMol Version 2.6-ucb 1.0. DS, distal site.**

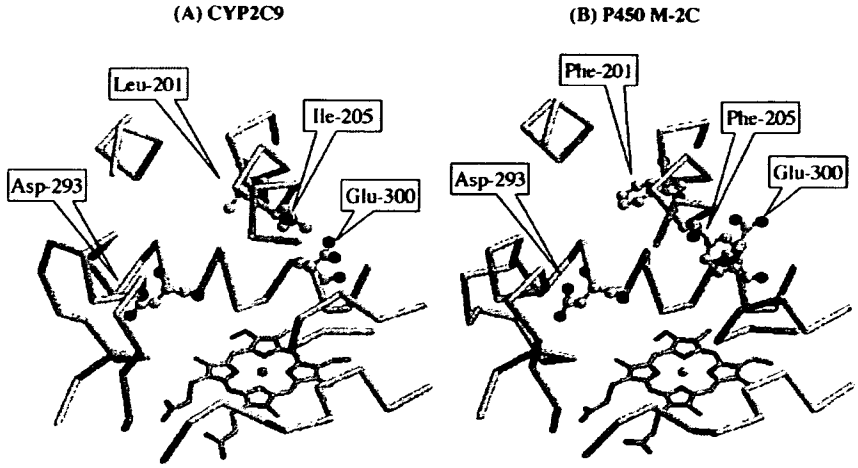


**Fig. 7 – Comparison of the active site structures between CYP2C9 (A) and P450 M-2C (B). Proteins are depicted as backbone form, and Phe-201 and Asp-293 for CYP2C8 and Phe-205 and Glu-300 for P450 M-2C as ball and stick form using RasMol Version 2.6-ucb 1.0.**

it possible that the *N*-benzoyl-3-phenylisoserine side-chain of PT binds to distal site 2, resulting in oxidation at the 6-position of the taxol ring.

The active site conformations of CYP2C8 and P450 M-2C which are shown with backbone depiction on RasMol are very similar (Fig. 6A and B). However, the shapes of the active site cavities of the two enzymes are considerably different from each other (Fig. 6C–F), especially, the shapes viewed from above (Fig. 6E and F) show clear differences in both distal sites 1 and 2. That is, the sizes of both distal sites 1 and 2 of CYP2C8 are larger than those of P450 M-2C. It is feasible that the smaller size of the active site cavity, particularly of the distal site 2 of P450 M-2C, makes it impossible for PT to appropriately dock in the active site, resulting in undetectable PT oxidation activity.

Fig. 7 shows the active sites of CYP2C9 (left panel) and P450 M-2C (right panel). The active site of CYP2C8 is almost the same as that of P450 M-2C. In the active site cavity of CYP2C9, there are two acidic amino acids, *i.e.*, Asp-293 and Glu-300, whose carboxylate groups may interact ionically with basic nitrogen atoms of TB. As a result, the *p*-methyl group of TB to be oxidized comes close to the heme iron, yielding *p*-hydroxymethyl-TB efficiently. In the active site cavity of P450 M-2C as well as of CYP2C8 having Asp-293 and Glu-300, however, there are two aromatic amino acids, Phe-201 and Phe-205. The phenyl group of Phe-205, in particular, is located just in front of the carboxylate group of Glu-300, which seems to block the ionic interaction between Glu-300 and the basic nitrogen atom of TB. Furthermore, these phenylalanine residues may cause hydrophobic interaction with the aromatic ring of TB, making the tolyl group of TB far from the heme ion, which may result in low capacities of P450 M-2C and CYP2C8 for TB *p*-methylhydroxylation.

In summary, we cloned a cDNA encoding a novel CYP2C enzyme, called P450 M-2C, from the marmoset liver. The deduced amino acid sequence showed high identities to human CYP2C8 (87%), CYP2C9 (78%) and CYP2C19 (77%). Yeast cell microsomal P450 M-2C catalyzed *p*-methylhydroxylation of only TB among four substrates, PT, DF, TB and S-MP, for human CYP2C enzymes. Marmoset liver microsomes exerted monophasic kinetics for TB, and its apparent $K_m$ value was similar to that of the recombinant P450 M-2C. Although three human recombinant CYP2C enzymes, CYP2C8, CYP2C9 and CYP2C19, also showed TB *p*-methylhydroxylation, the kinetic profile of CYP2C8 was most similar to that of P450 M-2C. TB oxidation by the marmoset microsomes and the recombinant P450 M-2C was similarly inhibited by quercetin, a CYP2C8 inhibitor. These results indicate that P450 M-2C (marmoset CYP2C8) is the major TB *p*-methylhydroxylase in the marmoset liver.

## Acknowledgments

This study was financially supported by a grant-in-aid for scientific research from the Ministry of Education, Science, Culture and Sports of Japan. We thank Miss Tomoko Sumada for her technical assistance.

## REFERENCES

[1] Rendic S, Di Carlo FJ. Human cytochrome P450 enzymes: a status report summarizing their reactions, substrates, inducers and inhibitors. Drug Metab Rev 1997;29:413–580.
[2] Evans WE, Relling MV. Pharmacogenomics: translating functional genomics into rational therapeutics. Science 1999;286:487–91.
[3] Parkinson A, Mudra DR, Johnson C, Dwyer A, Carroll M. The effects of gender, age, ethnicity, and liver cirrhosis on cytochrome P450 enzyme activity in human liver microsomes and inducibility in cultured human hepatocytes. Toxicol Appl Pharmacol 2004;199:193–209.
[4] Kastner M, Schulz-Schalge T, Neubert D. Purification and properties of cytochrome P-450 from liver microsomes of phenobarbital-treated marmoset monkeys (*Callithrix jacchus*). Toxicol Lett 1989;45:261–70.

[5] Sakuma T, Igarashi T, Hieda M, Ohgiya S, Isogai M, Ninomiya S, et al. Marmoset CYP1A2: primary structure and constitutive expression in livers. Carcinogenesis 1997;18:1985–91.
[6] Edwards RJ, Murray BP, Murray S, Schulz T, Neubert D, Gant TW, et al. Contribution of CYP1A1 and CYP1A2 to the activation of heterocyclic amines in monkeys and human. Carcinogenesis 1994;15:829–36.
[7] Schulz TG, Neubert D, Davies DS, Edwards RJ. Inducibility of cytochromes P-450 by dioxin in liver and extrahepatic tissues of the marmoset monkey (*Callithrix jacchus*). Biochim Biophys Acta 1996;1298:131–40.
[8] Schulz TG, Thiel R, Davies DS, Edwards RJ. Identification of CYP2E1 in marmoset monkey. Biochim Biophys Acta 1998;1382:287–94.
[9] Schulz TG, Thiel R, Neubert D, Brassil PJ, Schulz-Utermoehl T, Boobis AR, et al. Assessment of P450 induction in the marmoset monkey using targeted anti-peptide antibodies. Biochim Biophys Acta 2001;1546:143–55.
[10] Igarashi T, Sakuma T, Isogai M, Nagata R, Kamataki T. Marmoset liver cytochrome P450s: study for expression and molecular cloning of their cDNAs. Arch Biochem Biophys 1997;339:85–91.
[11] Narimatsu S, Oda M, Hichiya H, Isobe T, Asaoka K, Hanioka N, et al. Molecular cloning and functional analysis of cytochrome P450 1A2 from Japanese monkey liver: comparison with marmoset cytochrome P450 1A2. Chemico-biol Interact 2005;152:1–12.
[12] Hichiya H, Kuramoto S, Yamamoto S, Shinoda S, Hanioka N, Narimatsu S et al. Cloning and functional expression of a novel marmoset cytochrome P450 2D enzyme, CYP2D30: comparison with the known marmoset CYP2D19. Biochem Pharmacol 2004; 68:165–75.
[13] Narimatsu S, Yonemoto R, Saito K, Takaya K, Kumamoto T, Ishikawa T, et al. Oxidative metabolism of 5-methoxy-*N*,*N*-diisopropyltryptamine (Foxy) by human liver microsomes and recombinant cytochrome P450 enzymes. Biochem Pharmacol 2006;71:1377–85.
[14] Wan J, Imaoka S, Chow T, Hiroi T, Yabusaki Y, Funae Y. Expression of four rat CYP2D isoforms in *Saccharomyces cerevisiae* and their catalytic specificity. Arch Biochem Biophys 1997;348:383–90.
[15] Tsuzuki D, Takemi C, Yamamoto S, Tamagake K, Imaoka S, Funae Y, et al. Functional evaluation of cytochrome P450 2D6 with Gly42Arg substitution expressed in *Saccharomyces cerevisiae*. Pharmacogenetics 2001;11:709–18.
[16] Omura T, Sato R. The carbon monoxide-binding pigment of liver microsomes. I. Evidence for its hemoprotein nature. J Biol Chem 1964;239:2370–8.
[17] Narimatsu S, Gotoh M, Masubuchi Y, Horie Y, Ohmori S, Kitada M, et al. Stereoselectivity in bunitrolol 4-hydroxylation in liver microsomes from marmosets and Japanese monkeys. Biol Pharm Bull 1996;19:1429–33.
[18] Guengerich FP, Wang P, Davidson NK. Estimation of isozymes of microsomal cytochrome P-450 in rats, rabbits, and humans using immunochemical staining coupled with sodium dodecyl sulfate-polyacrylamide gel electrophoresis. Biochemistry 1982;21:1698–706.
[19] Soyama A, Saito Y, Hanioka N, Murayama N, Nakajima O, Katori N, et al. Non-synonumous single nucleotide alterations found in the CYP2C8 gene result in reduced in vitro paclitaxel metabolism. Biol Pharm Bull 2001;24: 1427–30.
[20] Schmitz G, Lepper H, Estler CJ. High-performance liquid chromatographic method for the routine determination of diclofenac and its hydroxy and methoxy metabolites from *in vitro* systems. J Chromatogr 1993;620:158–63.
[21] Komatsu K, Ito K, Nakajima Y, Kanamitsu S, Imaoka S, Funae Y, et al. Prediction of *in vivo* drug-drug interactions between tolbutamide and various sulfonamides in humans based on in vitro experiments. Drug Metab Dispos 2000;28:475–81.
[22] Nakajima M, Inoue T, Shimada N, Tokudome S, Yamamoto T, Kuroiwa Y. Cytochrome P450 2C9 catalyzes indomethacin O-demethylation in human liver microsomes. Drug Metab Dispos 1998;26:261–6.
[23] Lowry OH, Rosebrough NJ, Farr AL, Randall RJ. Protein measurement with the Folin phenol reagent. J Biol Chem 1951;193:265–75.
[24] Masuda K, Tamagake K, Katsu T, Torigoe F, Saito K, Hanioka N, et al. The roles of phenylalanine at position 120 and glutamic acid at position 222 in the oxidation of chiral substrates by cytochrome P450 2D6. Chirality 2006;18:167–76.
[25] Rahman A, Korzekwa KR, Grogan J, Gonzalez FJ, Harris JW. Selective biotransformation of taxol to 6α-hydroxytaxol by human cytochrome P450 2C8. Cancer Res 1994;54:5543–6.
[26] Mancy A, Dijols S, Poli S, Guengerich P, Mansuy D. Interaction of sulfaphenazole derivatives with human liver cytochromes P450 2C: molecular origin of the specific inhibitory effects of sulfaphenazole on CYP 2C9 and consequences for the substrate binding site topology of CYP 2C9. Biochemistry 1996;35:16205–12.
[27] Ko JW, Sukhova N, Thacker D, Chen P, Flockhart DA. Evaluation of omeprazole and lansoprazole as inhibitors of cytochrome P450 isoforms. Drug Metab Dispos 1997;25:853–62.
[28] Matsunaga T, Ohmori S, Ishida M, Sakamoto Y, Nakasa H, Kitada M. Molecular cloning of monkey CYP2C43 cDNA and expression in yeast. Drug Metab Pharmacokinet 2002;17:117–24.
[29] Lasker JM, Wester MR, Aramsombatdee E, Raucy JL. Characterization of CYP2C19 and CYP2C9 from human liver: respective roles in microsomal tolbutamide, S-mephenytoin, and omeprazole hydroxylations. Arch Biochem Biophys 1998;353:16–28.
[30] Flanagan JU, McLaughlin LA, Paine MJ, Sutcliffe MJ, Roberts GC, Wolf CR. Role of conserved Asp293 of cytochrome P450 2C9 in substrate recognition and catalytic activity. Biochem J 2003;370:921–6.
[31] Tanaka T, Kamiguchi N, Okuda T, Yamamoto Y. Characterization of the CYP2C8 active site by homology modeling. Chem Pharm Bull 2004;52:836–41.

Drug Metab. Pharmacokinet. 21 (4): *SNP30* (337)–*SNP39* (346) (2006).

## SNP Communication

# *Novel Genetic Variations and Haplotypes of Hepatocyte Nuclear Factor 4α (HNF4A) Found in Japanese Type II Diabetic Patients*

Hiromi FUKUSHIMA-UESAKA[1,2], Yoshiro SAITO[1,2,*], Keiko MAEKAWA[1,2], Mayumi SAEKI[1], Naoyuki KAMATANI[3], Hiroshi KAJIO[4], Nobuaki KUZUYA[4], Kazuki YASUDA[5] and Jun-ichi SAWADA[1,2]

[1]*Project Team for Pharmacogenetics,* [2]*Division of Biochemistry and Immunochemistry, National Institute of Health Sciences, Tokyo, Japan;* [3]*Division of Genomic Medicine, Department of Advanced Biomedical Engineering and Science, Tokyo Women's Medical University, Tokyo, Japan;* [4]*Division of Endocrine and Metabolic Diseases, the Hospital,* [5]*Department of Metabolic Disorder, Research Institute, International Medical Center of Japan, Tokyo, Japan*

Full text of this paper is available at http://www.jstage.jst.go.jp/browse/dmpk

**Summary:** Thirty-nine single nucleotide variations, including 16 novel ones, were found in the 5′ promoter region, all of the exons and their surrounding introns of *HNF4A* in 74 Japanese type II diabetic patients. The following novel variations were identified (based on the amino acid numbering of splicing variant 2): −208G>C in the 5′ promoter region; 1154C>T (A385V) and 1193T>C (M398T) in the coding exons; 1580G>A, 1852G>T, 2180C>T, 2190G>A, and 2362_2380delAAGAATGGTGTGGGAGAGG in the 3′-untranslated region, and IVS1+231G>A, IVS2−83C>T, IVS3+50C>T, IVS3−54delC, IVS5+173_176delTTAG, IVS5−181_−180delAT, IVS8−106A>G, and IVS9−151A>C in the introns. The allele frequencies were 0.311 for 2362_2380delAAGAATGGTGTGGGAGAGG, 0.054 for 1580G>A, 0.047 for 1852G>T, 0.020 for IVS1+231G>A, 0.014 for IVS9−151A>C, and 0.007 for the other 11 variations. In addition, one known nonsynonymous single nucleotide polymorphism, 416C>T (T139I), was detected at a 0.007 frequency. Based on the linkage disequilibrium profiles, the region analyzed was divided into three blocks. Haplotype analysis determined/inferred 10, 16, and 12 haplotypes for block 1, 2, and 3, respectively. Our results on *HNF4A* variations and haplotypes would be useful for pharmacogenetic studies in Japanese.

**Key words:** ***HNF4A*; genetic variation; amino acid alteration; haplotype**

## Introduction

Hepatocyte nuclear factor 4α is an orphan nuclear receptor. This transcriptional factor is predominantly expressed in the liver, small intestine, colon, kidney, and pancreas and acts as a homodimer.[1] To date, nine transcript variants have been reported with alternative initiation and splicing of four exon 1's, and alternative splicing in exons 8–10.[2] As for the exon 1's, 6 isoforms (isoforms 1–6) are transcribed from exon 1A with the P1 promoter. Isoforms 4–6 use additional exon 1B, which confer an extra 30 amino acids as compared with the corresponding isoforms 1–3. The transcription of 3 isoforms (isoforms 7–9) starts from exon 1D with the P2 promoter approximately 45 kb upstream of exon 1A.[3] Isoforms 2, 5, and 8 use the alternative splice donor site in exon 9, 30 bases downstream of the site of isoforms 1, 4, and 7, and thus are alternatively spliced forms of isoforms 1, 4, and 7. On the other hand, the isoforms 3, 6, and 9 utilize exon 8 with a 125-base extension,

On Dec. 8, 2005, novel variations were not reported in the databases of the Japanese Single Nucleotide Polymorphisms (JSNP) (http://snp.ims.u-tokyo.ac.jp/), dbSNP in the National Center for Biotechnology Information (http://www.ncbi.nlm.nih.gov/SNP/), or PharmGKB (http://www.pharmgkb.org/do/).

*Received; December 12, 2005, Accepted; March 9, 2006*

**To whom correspondence should be addressed*: Yoshiro SAITO, Ph.D., *Division of Biochemistry and Immunochemistry, National Institute of Health Sciences, 1-18-1 Kamiyoga, Setagaya-ku, Tokyo 158-8501, Japan. Tel. +81-3-5717-3831, Fax. +81-3-5717-3832, E-mail: yoshiro@nihs.go.jp*

resulting in an early stop codon in exon 8.[4] The mRNA level of isoform 1 or 2 was reported to be higher than that of isoform 3 in the liver.[4] Variant 4, and probably 5 and 6, has no detectable transactivation potential.[1] The transcription of HNF4$\alpha$ mainly initiates at the P1 promoter in adult liver and kidney.[2,3] In the pancreas, the transcription starts from the P2 promoter,[2,3] though one report showed mRNA expression of isoforms 1 and 2 in pancreatic islets and $\beta$ cells.[5]

Human HNF4$\alpha$ protein can be divided into 6 domains named domains A (the N-terminal domain) to F (the C-terminal domain).[1,6] Domains A and B (amino acid residues 1–60 based on isoform 2) contain a ligand-independent transactivation function AF-1. Domains C (61–126) and D (127–143) are important for DNA-binding and full transcriptional activity, respectively. Domain E (144–378) contains a ligand-binding domain and a ligand-dependent transactivation function AF-2. The domains D and E are also important for functional interactions with co-activators such as PGC-1 and SRC-3.[7] Domain F (379–474) has been shown to inhibit the transactivation potential of AF-2.[6] In addition, it was reported that isoform 8 showed markedly reduced transcriptional activity compared to isoform 2, probably due to lack of AF-1 activity by usage of exon 1D, instead of exon 1A.[5,8]

Nuclear factor HNF4$\alpha$ has been reported to be involved in the induction of many drug metabolizing enzymes, such as *CYP2C9*, *CYP2C8*, *CYP2A6*, *CYP3A4*, and *UGT1A9* with known binding sites.[9–13] Interindividual differences in mRNA, protein, and activity levels have been shown in these drug metabolizing enzymes, and several genetic variations with functional significance have been found. Presently, however, the reported variations in these genes do not fully explain the interindividual differences. It may be possible that genetic variations of *HNF4A* may contribute to these differences. In the present study, the 5′-regulatory region, all the exons (except for non-functional exons 1B and 1C, and pancreatic exon 1D), and their surrounding introns of *HNF4A* were sequenced in 74 Japanese patients. Sixteen novel variations, including two nonsynonymous ones, were identified.

## Materials and Methods

**Human genomic DNA samples:** DNA was extracted from the blood leukocytes of 74 Japanese type II diabetic patients who had received glimepiride. The ethical review boards of the International Medical Center of Japan and the National Institute of Health Sciences approved this study. Written informed consent was obtained from all participating patients.

**Polymerase chain reaction (PCR) conditions for DNA sequencing:** First, multiplex PCR was performed to amplify the entire *HNF4A* gene with two mixed primer sets (Mix 1 and Mix 2 in "1st PCR" in **Table 1**). Amplification was performed from 50 ng of genomic DNA using 1 unit of Ex-Taq (Takara Bio. Inc, Shiga, Japan) with 0.2 $\mu$M of the mixed primers sets. The first PCR conditions were 94°C for 5 min, followed by 30 cycles of 94°C for 30 sec, 60°C for 1 min, and 72°C for 2 min, and then a final extension at 72°C for 7 min. After the PCR products were treated with a PCR Product Pre-Sequencing Kit (USB Co., Cleveland, OH, USA), each exon was amplified separately using one-fifth of the volume of the 1st PCR product as a template by Ex-Taq (0.1 units) with a set of primers (0.2 $\mu$M) listed in "2nd PCR" of **Table 1** (designed in the intronic regions, except for exon 10, which is described below). The second-round PCR conditions were 94°C for 5 min, followed by 30 cycles of 94°C for 30 sec, 60°C for 1 min, and 72°C for 2 min, and then a final extension at 72°C for 7 min. Next, the PCR products were treated with a PCR Product Pre-Sequencing Kit and directly sequenced on both strands using an ABI BigDye Terminator Cycle Sequencing Kit (Applied Biosystems, Foster City, CA, USA) with the primers listed in "Sequencing" of **Table 1**. The excess dye was removed by a DyeEx96 kit (Qiagen, Hilden, Germany). The eluates were analyzed on an ABI Prism 3730 DNA Analyzer (Applied Biosystems). All detected rare variations were confirmed by repeating the PCR from the genomic DNA and sequencing the newly generated PCR products. Since exon 10 spans approximately 1.9 kb, the exon was amplified in two fragments in the 2nd PCR and sequenced with five forward and four reverse primers.

**Linkage disequilibrium (LD) and haplotype analyses:** Hardy-Weinberg equilibrium and LD analysis was performed by SNPAlyze software (Dynacom Co., Yokohama, Japan), and pairwise LD between variations was analyzed using $r^2$ and $|D'|$ values. For $|D'|$ values, the variations detected with a frequency greater than 0.05 were used. Based on the LD analysis, we divided the variations into 3 gene blocks and estimated haplotypes for each block. Some of the haplotypes were unambiguous from subjects with homozygous variations at all sites or a heterozygous variation at only one site. Separately, the diplotype configurations (a combination of haplotypes) were inferred by LDSUPPORT software, which determines the posterior probability distribution of the diplotype configuration for each subject based on the estimated haplotype frequencies.[14] The haplotypes inferred in single subjects are described with haplotype names and a question mark in **Tables 3 to 5**, since the predictability for these very rare haplotypes is known to be low in some cases. The haplotypes detected in this study were tentatively named as numbers plus small alphabetical letters. The block 2 **3a*